Biotechnology Advances 27 (2009) 153–176

Contents lists available at ScienceDirect

Biotechnology Advances

journal homepage: www.elsevier.com/locate/biotechadv

Research review paper

Bioreactor scale-up and oxygen transfer rate in microbial processes: An overview

Felix Garcia-Ochoa *, Emilio Gomez

Dept. Ingeniería Química. Facultad Químicas. Universidad Complutense. 28040-Madrid, Spain

ARTICLE INFO

Article history:
Received 21 May 2008
Received in revised form 18 October 2008
Accepted 26 October 2008
Available online 12 November 2008

Keywords:
Oxygen transfer rate
Bioreactors scale-up
Microbial processes
Gas–liquid interface

ABSTRACT

In aerobic bioprocesses, oxygen is a key substrate; due to its low solubility in broths (aqueous solutions), a continuous supply is needed. The oxygen transfer rate (OTR) must be known, and if possible predicted to achieve an optimum design operation and scale-up of bioreactors. Many studies have been conducted to enhance the efficiency of oxygen transfer. The dissolved oxygen concentration in a suspension of aerobic microorganisms depends on the rate of oxygen transfer from the gas phase to the liquid, on the rate at which oxygen is transported into the cells (where it is consumed), and on the oxygen uptake rate (OUR) by the microorganism for growth, maintenance and production.

The gas–liquid mass transfer in a bioprocess is strongly influenced by the hydrodynamic conditions in the bioreactors. These conditions are known to be a function of energy dissipation that depends on the operational conditions, the physicochemical properties of the culture, the geometrical parameters of the bioreactor and also on the presence of oxygen consuming cells.

Stirred tank and bubble column (of various types) bioreactors are widely used in a large variety of bioprocesses (such as aerobic fermentation and biological wastewater treatments, among others). Stirred tanks bioreactors provide high values of mass and heat transfer rates and excellent mixing. In these systems, a high number of variables affect the mass transfer and mixing, but the most important among them are stirrer speed, type and number of stirrers and gas flow rate used. In bubble columns and airlifts, the low-shear environment compared to the stirred tanks has enabled successful cultivation of shear sensitive and filamentous cells. Oxygen transfer is often the rate-limiting step in the aerobic bioprocess due to the low solubility of oxygen in the medium. The correct measurement and/or prediction of the volumetric mass transfer coefficient, (k_La), is a crucial step in the design, operation and scale-up of bioreactors.

The present work is aimed at the reviewing of the oxygen transfer rate (OTR) in bioprocesses to provide a better knowledge about the selection, design, scale-up and development of bioreactors. First, the most used measuring methods are revised; then the main empirical equations, including those using dimensionless numbers, are considered. The possible increasing on OTR due to the oxygen consumption by the cells is taken into account through the use of the biological enhancement factor. Theoretical predictions of both the volumetric mass transfer coefficient and the enhancement factor that have been recently proposed are described; finally, different criteria for bioreactor scale-up are considered in the light of the influence of OTR and OUR affecting the dissolved oxygen concentration in real bioprocess.

Contents

* Corresponding author.
E-mail address: fgochoa@quim.ucm.es (F. Garcia-Ochoa).

0734-9750/$ – see front matter © 2008 Elsevier Inc. All rights reserved.
doi:10.1016/j.biotechadv.2008.10.006

1. Introduction

Most industrial microbial processes are aerobic, and are mostly carried out in aqueous medium containing salts and organic substances; usually these broths are viscous, showing a non-Newtonian behavior. In these processes, oxygen is an important nutrient that is used by microorganisms for growth, maintenance and metabolite production, and scarcity of oxygen affects the process performance (Garcia-Ochoa et al., 2000a; Calik et al., 2004; Liu et al., 2006a). Therefore, it is important to ensure an adequate delivery of oxygen from a gas stream to the culture broth. Consequently, accurate estimtion of the oxygen transfer rate (OTR) at different scales and under different operational conditions has a relevant role for the prediction of the metabolic pathway for both growth and production of any wished metabolite in the aerobic cultus it is of critical importance for the selection, design and scale-up of bioreactors.

Extensive literature on the oxygen transfer rate in bioreactors is nowadays available and a considerable part of it has been published in the last years (Arrua et al., 1990; Badino et al., 2001; Galaction et al., 2004; Puthli et al., 2005; Clarke et al., 2006). Substantial results on different aspects of oxygen transport have been reviewed in different works (Margaritis and Zajic, 1978; Kawase and Moo-Young, 1990; Arjunwadkar et al., 1998; Gogate et al., 2000; Kilonzo and Margaritis, 2004; Clarke and Correia, 2008).

The oxygen mass transfer rate can be described as proportional to the concentration gradient, being the volumetric mass transfer coefficient, k_La (Eq. (4)) the proportionality constant. The maximum value of the concentration gradient is limited due to the low solubility of most gases associated to aerobic fermentation, notably oxygen. Therefore, the maximum mass transfer rate from the gas to the liquid in the bioreactor can be estimated by the product $k_La{\cdot}C^*$, being C^* the saturation concentration in the liquid phase.

There are a great number of empirical equations to determine k_La, and efforts have recently been made for theoretical prediction of k_La values; most of these works having been developed for bubble columns and airlifts (Kawase et al., 1987; Garcia-Calvo, 1989; Kawase et al., 1992a,b; Garcia-Calvo, 1992; Tobajas et al., 1999; Sanchez et al., 2000), and a lesser number dealing with the transport in stirred tanks bioreactors (Kawase and Moo-Young, 1988; Kawase et al., 1992a; Garcia-Ochoa and Gomez, 2004, 2005). These prediction methods successfully predict the transport coefficient for bioreactors of different sizes and under different operational conditions.

The bioprocesses are usually conducted under previously optimized conditions (temperature, pH, pressure, mixing, concentrations of biomass and nutrients), with an operational mode previously chosen (batch, fed-batch, resting cell, continuous). The overall mass transfer rate is not easy to measure, because different phenomena are simultaneously taking place; also the relative importance of these phenomena changes with the scale, the type of bioreactor, etc. Therefore, the OTR is influenced by a high number of parameters (physical properties of gas and liquid, operational conditions, geometrical parameters of the bioreactor) and also by the presence of biomass, that is, the consumption of oxygen by the cells. Fig. 1 is a schematic view of the different factors affecting OTR at different levels in a bioprocess; these factors will be discussed in this review.

Bioprocesses involve simultaneous transport and biochemical reactions of several chemical species. Sometimes, the transport of substrates to cells occurs at a rate considerably higher than the rate of the metabolic biochemical reactions; in this case, the overall rate of substrate conversion is governed only by the kinetics of the biochemical reactions. However, if mass transfer rate is lower than reaction rate, transport rate can be the step controlling the overall process rate and, moreover, the mass transfer rate may be influenced by the chemical rate of the bioprocess. When a species in gas phase is absorbed into a liquid and reacts there, the concentration profiles of the absorbed species change due to the chemical reaction and the absorption rate may be enhanced (Van Swaaij and Versteeg, 1992; Benbelkacem and Debellefontaine, 2003). Oxygen absorption into a fermentation broth can be considered as the absorption of a gas into a liquid where it reacts, oxygen is consumed by the suspended microorganism, and therefore an enhancement of oxygen mass transfer rate can take place (Tsao, 1969; Merchuk, 1977; Ju and Sundararajan, 1992; Garcia-Ochoa and Gomez, 2005). The increase of the specific gas absorption rate per driving force unit and per interfacial area unit, due to the presence of the dispersed phase (in this case the microorganism), can be characterized by an enhancement factor, E.

The aim of this work is to examine the oxygen transfer in microbial processes in different bioreactors (stirred tanks and bubble columns), taking into account the effects of changes in viscosity, addition of

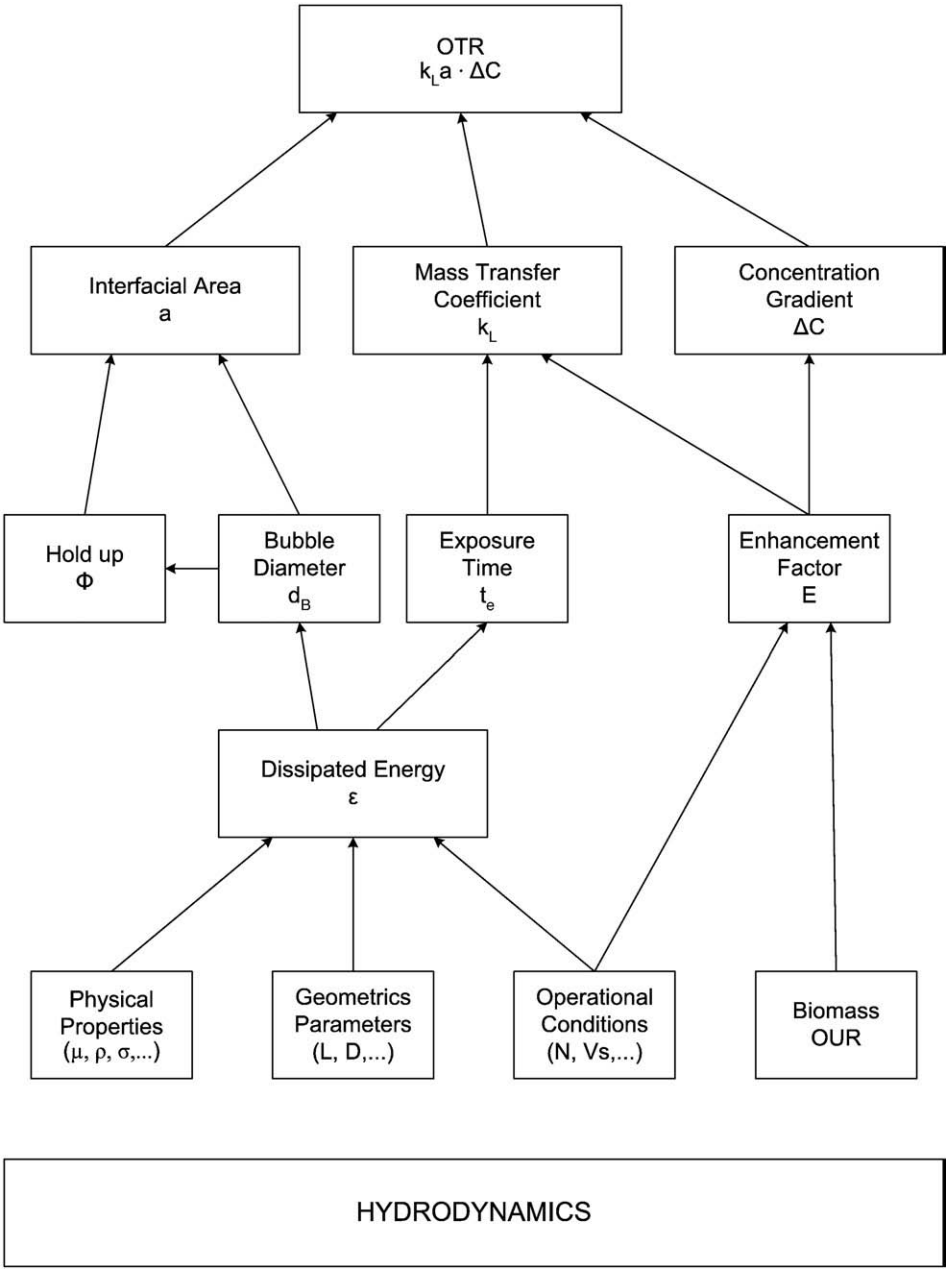

Fig. 1. Relationship between OTR, volumetric mass transfer coefficient and hydrodynamic parameters in bioreactors at several levels.

substances able to change the hydrodynamics (salts, sugars, surfactants, anti-foam, etc.), together with other special aspects of bioreactors such as oxygen consumption by the microorganism.

1.1. Oxygen transfer rate (OTR) description

During aerobic bioprocess, the oxygen is transferred from a rising gas bubble into a liquid phase and ultimately to the site of oxidative phosphorylation inside the cell, which can be considered as a solid particle. The transport of oxygen from air bubbles to the cells can be represented by a number of steps and resistances, as schematized in Fig. 2; the liquid film resistances around bubbles usually control the overall transfer rate.

The simplest theory on gas–liquid mass transfer is the two film model (Whitman, 1923) and usually the gas–liquid mass transfer rate is modeled according to this theory (see Fig. 3), describing the flux through each film as the product of the driving force by the mass transfer coefficient, according to:

$$J^0 = k_G \cdot (p_G - p_i) = k_L \cdot (C_i - C_L) \quad (1)$$

being J^0 the molar flux of oxygen ($mol \cdot m^{-2}\ s^{-1}$) through the gas–liquid interface; k_G and k_L, are the local mass transfer coefficients; p_G is the oxygen partial pressure in the gas bubble; and C_L, the dissolved oxygen concentration in the bulk liquid; index i refers to values at the gas–liquid interface.

Since the interfacial concentrations are not directly measurable and considering the overall mass transfer coefficient, it can be rewritten:

$$J^0 = K_G\left(p_G - p^*\right) = K_L\left(C^* - C_L\right) \quad (2)$$

where p^* is the oxygen pressure in equilibrium with liquid phase; C^* is the oxygen saturation concentration in the bulk liquid in

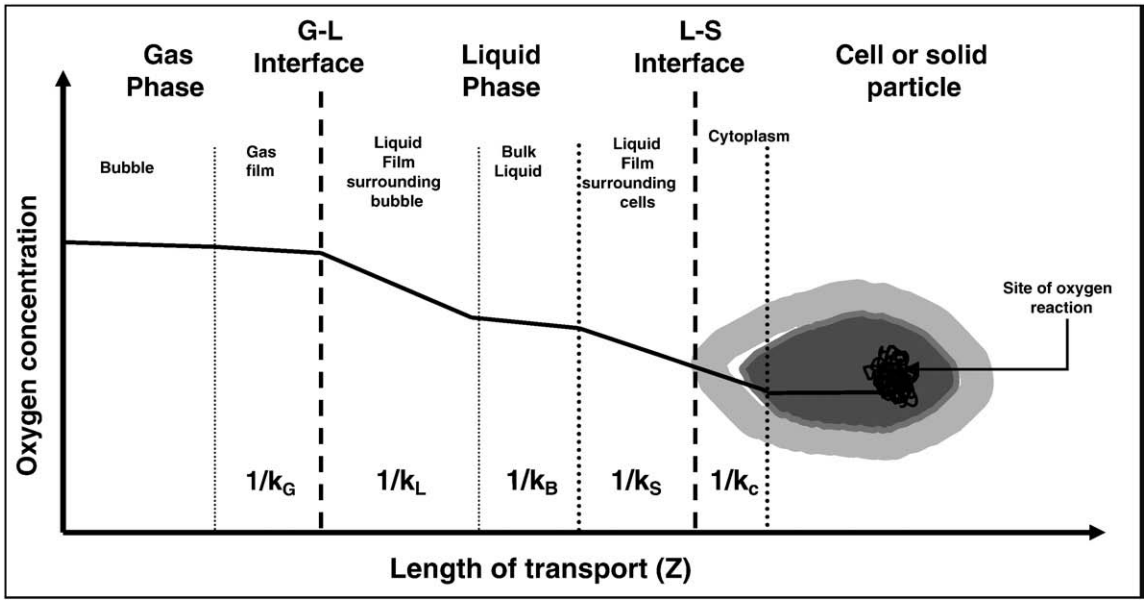

Fig. 2. Steps and resistances for oxygen transfer from gas bubble to cell. (i) transfer from the interior of the bubble and gas film; (ii) movement across the gas–liquid interface; (iii) diffusion through the relatively stagnant liquid film surrounding the bubble; (iv) transport through the bulk liquid; (v) diffusion through the relatively stagnant liquid film surrounding the cells; (vi) movement across the liquid-cell interface; and (vii) transport through the cytoplasm to the site of biochemical reaction.

equilibrium to the bulk gas phase, according to Henry's law ($p^*=HC^*$); K_G and K_L are the overall mass transfer coefficients.

Combining Eqs. (1) and (2), the following relationship is obtained:

$$\frac{1}{K_L} = \frac{1}{Hk_G} + \frac{1}{k_L} \tag{3}$$

Taking into account that oxygen is only slightly soluble in water (H is very large), it is commonly accepted that the greatest resistance for mass transfer is on the liquid side of the interface and the gas phase resistance can usually be neglected and thus the overall mass transport coefficient is equal to the local coefficient: $K_L=k_L$.

The oxygen mass transfer rate per unit of reactor volume, N_{O2}, is obtained multiplying the overall flux by the gas–liquid interfacial area per unit of liquid volume, a:

$$N_{O_2} = a \cdot J^0 = k_L a \cdot \left(C^* - C_L\right) \tag{4}$$

Due to the difficulty of measuring k_L and a separately, usually the product k_La is measured and this parameter – called volumetric mass transfer coefficient – characterizes the transport from gas to liquid.

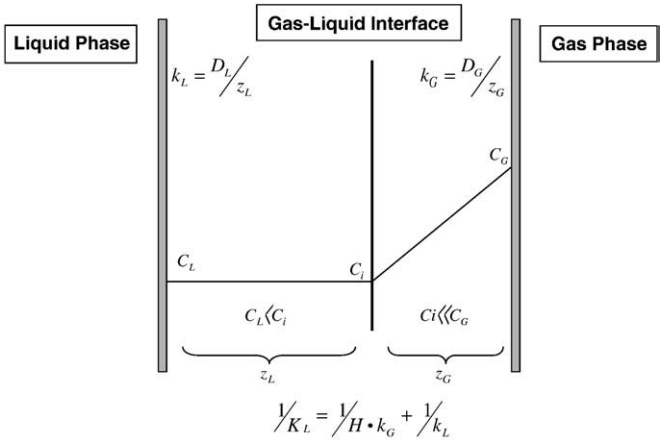

Fig. 3. Schematic representation of the gas–liquid interface, concentrations and mass transfer coefficients K_L, k_L and k_G according to film theory.

The driving force is the gradient between the concentration of the oxygen at the interface and that in the bulk liquid (average concentration). Factors affecting this gradient include the solubility and metabolic activity. The gas solubility, C^*, in electrolyte solutions is usually smaller than the gas solubility in pure water ("salting-out effect"). Gas solubility is mainly dependent on the temperature, the pressure, concentration and type of salts present and the chemical reactions (Linek and Vacek, 1981a; Hermann et al., 1995; Weissenborn and Pugh, 1996).

2. Experimental determination of the volumetric mass transfer coefficient (k_La)

The determination of k_La in bioreactors is essential in order to establish aeration efficiency and to quantify the effects of the operating variables on the provision of dissolved oxygen. A number of methods have been developed to determine the oxygen transfer rate in bioreactors (Van't Riet, 1979). Some of these methods are applied to others compounds as well, but others are specific for oxygen transfer measurement. When selecting a method, several factors must be taken into account (Novak and Klekner, 1988):

i. the aeration and homogenization systems used,
ii. the bioreactor type and its mechanical design,
iii. the composition of the fermentation medium and
iv. the possible effect of the presence of microorganism.

The mass balance for the dissolved oxygen in the well-mixed liquid phase can be established as:

$$\frac{dC}{dt} = \text{OTR} - \text{OUR} \tag{5}$$

where dC/dt is the accumulation oxygen rate in the liquid phase, OTR represents the oxygen transfer rate from the gas to the liquid, described according to Eq. (4), and OUR is the oxygen uptake rate by the microorganisms; this last term can be expresed by the product $q_{O2}{\cdot}C_X$, being q_{O2} the specific oxygen uptake rate of the microorganism employed and C_X the biomass concentration.

The most common methods applied to measuring the oxygen transfer rate in a microbial bioprocess can be classified depending on

whether the measurement is realized in the absence of microorganisms or with dead cells or in the presence of biomass that consumes oxygen at the time of measurement.

2.1. Measuring methods of k_La without biological consumption of oxygen

In the absence of biomass or with non-respiring cells, when biochemical reactions do not take place, OUR=0. In this case, Eq. (5) can be simplified to:

$$\frac{dC}{dt} = k_L a \cdot \left(C^* - C\right) \tag{6}$$

Some measuring methods are based on Eq. (6) and different techniques from measuring the dissolved oxygen concentration can be used, herein divided into chemical and physical methods.

2.2. Chemical methods

Chemical methods were the first to become widely accepted. In general, however, these methods are not recommended for volumetric mass transfer coefficient determination in the case of sparged bioreactors, due to the changes of physicochemical properties of liquids, especially coalescence, produced by the addition of chemicals. This method can give values higher than the real ones, because the absorption rate may be enhanced by fast chemical reactions in the liquid phase, if the experimental conditions are not kept within certain limits.

2.3. Sodium sulfite oxidation method

This method is based on the reaction of sodium sulfite, a reducing agent, with the dissolved oxygen to produce sulfate, in the presence of a catalyst (usually a divalent cation of Cu^{++} or Co^{++}) (Cooper et al., 1944); the reaction can be expressed as:

$$2\ SO_4^{-2} - O_2 - 2\ SO_3^{-2} = 0 \tag{7}$$

There is a concentration range of sodium sulfite (from 0.04 to 1 N) for which the reaction is so fast that oxygen concentration can be assumed to be zero. The reaction rate is much faster than the oxygen transfer rate; therefore, the rate of oxidation is controlled by the rate of mass transfer, and measuring the overall rate, the mass transport rate can be determined. The reaction rate is a complex function of the catalyst concentration and the operational conditions that must be controlled in order to obtain reproducible measurements (Linek and Vacek, 1981b).

The experimental procedure consists in first filling the bioreactor with a 1 N sodium sulfite solution containing at least 10^{-3} M of Cu^{2+} ion, turning on the air and starting the time when the air emerges from the sparger; allowing the oxidation reaction to continue for some minutes; after that, stopping the air flow, agitating, and taking samples of known volumes at regular time intervals. Mixing each sample with an excess of standard iodine reagent and finally titrating with standard sodium tiosulfate solution ($Na_2S_2O_3$) to a starch indicator end point. The reactions are:

$$SO_4^{-2} + 2H^+ + 2I^- - SO_3^{-2} - I_2 - H_2O = 0 \tag{8}$$

$$S_4O_6^{2-} + 2I^- - 2S_2O_3^{2-} - I_2 = 0 \tag{9}$$

The amount of residual sulfite can be also estimated indirectly by the stoichiometry of the reaction (8) on basis of colorimetric determination of the iodine concentration (Yang and Wang, 1992).

Once the sulfite concentration is measured versus time, the rate of sulfite consumption is determined and k_La may be calculated from:

$$-\frac{dC_{Na_2SO_3}}{dt} = 2k_L a C^* \tag{10}$$

As quoted above, this reaction is catalyzed by heavy metal ions, usually Co^{++}; the concentration of these ions must be kept carefully within narrow boundaries ($5\cdot10^{-6}$ M) in order to obtain an adequate reaction rate, avoiding acceleration of oxygen uptake due to the chemical reaction. Linek and Vacek (1981b) have reviewed the use of the sulfite oxidation method, as a model reaction of known kinetics, and its capacity for accurately determining mass transfer characteristics. The sodium sulfite oxidation method is relatively easy to carry out. This technique has been used in a large number of works (Dussap et al., 1985; Ogut and Hatch, 1988; Thibault et al., 1990; Yasukawa et al., 1991; Yang and Wang, 1992; Benadda et al., 1997; Garcia-Ochoa and Gomez, 1998; Liu et al., 2006a). However, this method has the limitation that, because some of its physicochemical properties are very different from those of fermentation broths, the hydrodynamics of the solution is changed, mainly due to the influence of those properties on bubble size. These changes cause the k_La values obtained to be bigger than those obtained by other techniques, and non realistic (Van't Riet, 1979; Garcia-Ochoa and Gomez, 1998).

2.4. Absorption of CO_2

This method was proposed by Danckwerts and Gillham (1966). The method consists in the absorption of carbon dioxide in an alkaline solution. The reactions taking place are:

$$HCO_3^- - CO_2 - OH^- = 0 \tag{11}$$

$$HCO_3^- + H^+ - CO_2 - H_2O = 0 \tag{12}$$

According to Danckwerts (1970), the reaction expressed by Eq. (11) is of second order kinetics:

$$r = k \cdot [CO_2] \cdot [OH^-] \tag{13}$$

the constant rate (20 °C) takes a value of $5\cdot10^3$ $L\cdot mol^{-1}\cdot s^{-1}$:

On the other hand, reaction (12) has a first order kinetic equation:

$$r' = k' \cdot [CO_2] \tag{14}$$

the constant rate (20 °C) takes a value of de $2\cdot10^{-2}$ s^{-1}.

Therefore, in any solution in which the concentration of OH^- is higher than 10^{-4} $mol\cdot L^{-1}$ (pH>10), the rate of reaction (11) will have a constant rate of pseudo-first order of, at least, 0.5 s^{-1}, twenty-five times higher than the rate constant of Eq. (12). Therefore, it is possible to assume that the reaction (12) is the controlling step determining the absorption rate of carbon dioxide in basic solutions with pH>10.

In order to be able to apply this method it is necessary to work with a reaction of first order, whereas the reaction (12) is of second order. However, for gases in which the partial pressure of CO_2 is not high, the reaction behaves like one of pseudo-first order (Sharma and Danckwerts, 1970) and the mass transfer coefficient can be obtained from:

$$-\frac{1}{2}\frac{dC_{CO_2}}{dt} = k_L a \cdot C^* \sqrt{k \cdot C_{CO_2}} \tag{15}$$

In principle, this method uses a reaction more easily controllable than the previous method, the oxidation of sulfite. Nevertheless, it has disadvantages similar to the previous one, due to the need of using high concentrations of the ion OH^- that inhibits the coalescence of the bubbles.

To quantify the gas liquid mass transfer of other compounds, such as oxygen, the relationship between the volumetric mass transfer coefficients for two different compounds, according to film theory, can be employed:

$$\frac{k_L a|_{O_2}}{k_L a|_{CO_2}} = \frac{D_{O_2}}{D_{CO_2}} \tag{16}$$

2.5. Physical methods

The physical methods employ the response of oxygen probe to concentration changes in the dispersed gas in the medium, under non-stationary conditions. These methods are nowadays the most commonly used for oxygen transfer estimation, as they are based on the measurement of dissolved oxygen concentration in the liquid during the absorption or desorption of oxygen in the solution (Dussap et al., 1985; Baird et al., 1993; Nocentini et al., 1993; Merchuk et al., 1994; Garcia-Ochoa and Gomez, 1998; Sanchez et al., 2000; Puthli et al., 2005; Clarke et al., 2006; Zhan et al., 2006).

2.6. Dynamic method

The dynamic method is one of those based on the measurement of dissolved oxygen concentration in the medium by absorption o desorption of oxygen. After a step change in the concentration in the inlet gas, the dynamic change in the dissolved oxygen concentration is analyzed. In this method, Eq. (5) can again be used, being now OUR = 0, which integration results (between two different times):

$$\ln\frac{C^* - C_2}{C^* - C_1} = -k_L a \cdot (t_2 - t_1) \tag{17}$$

The dynamic technique of absorption consists of producing the elimination of oxygen in the liquid phase, for example by means of bubbling nitrogen or by the addition of sodium sulfite, until the oxygen concentration is equal to zero. Later, the liquid is put in contact again with air, measuring the variation (increase) of the oxygen concentration with time.

The dynamic technique desorption consists in supplying air until the oxygen saturation concentration in the liquid is reached. Then, nitrogen is introduced downwards into the vessel and the dissolved oxygen concentration decrease is recorded as a function of time. Under these conditions: $t_1 = 0$, $C_1 = C_{Lo}$, Eq. (17) can be expressed as:

$$\ln\left(\frac{C_{Lo}}{C_L}\right) = k_L a \cdot t \tag{18}$$

On the other hand, when the oxygen has been desorbed of culture (by supply of nitrogen, e.g.) and oxygen is again supplied, now $C_1 = 0$ at $t_1 = 0$, Eq. (17) can be expressed as:

$$\ln\left(1 - \frac{C_L}{C^*}\right) = -k_L a \cdot t \tag{19}$$

Eqs. (18) and (19) describe the time course of dissolved oxygen from the restart of aeration or when it is eliminated from the culture; in both cases, $k_L a$ can be determined from the slope of the $ln\, f(C_L)$ vs. time graph (see Fig. 4 as an example).

This technique is interesting for studying the influence of operational conditions on the volumetric mass transfer coefficient, and is widely employed in the literature (Garcia-Ochoa and Gomez, 1998; Sanchez et al., 2000; Puthli et al., 2005; Djelal et al., 2006). Nevertheless, it is necessary to take into account that the response time of the electrode, τ_r, is a critical parameter for the determination of accuracy values of oxygen concentration. This response can affect the correct determination of the mass transfer coefficient if the time

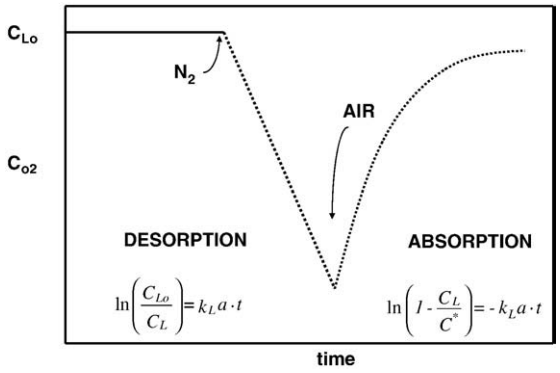

Fig. 4. Schematic description of the dynamic technique desorption–absorption of oxygen for inert condition measurements.

characteristic for the oxygen transport, $1/k_L a$, is of the same order than the response time of the electrode, defined as the time necessary to reach 63% of the final value measured when exposed to a step change of concentration (Van't Riet, 1979). The response time of the electrode can be determined by transferring the oxygen electrode from a solution with sodium sulfite (whose oxygen concentration is zero) to another dissolution saturated with air (100% of saturation). In the case when the electrode of oxygen has a high value of τ_r it would be necessary to introduce a correction in the response model (Eq. (6)); a good approach is a first order dynamic (Weiland and Onken, 1981; Godbole et al., 1984), according to:

$$\frac{dC_{me}}{dt} = \frac{(C_L - C_{me})}{\tau_r} \tag{20}$$

The combination of Eqs. (6) and (20) permits to obtain the value of $k_L a$ from the dissolved oxygen concentration measurements in case of saturation, according to the following equation:

$$C_{me} = C^* + \frac{C^* - C_0}{1 - \tau_r k_L a} \cdot \left[\tau_r k_L a \exp\left(\frac{-t}{\tau_r}\right) - \exp(-k_L a \cdot t)\right] \tag{21}$$

where C_{me} is the oxygen concentration measured by the electrode and C_0 is the oxygen concentration at the initial time of the aeration.

Assuming that the dynamic response of the electrode is of first order, characterized by a constant time, a simple criterion for the suitable selection of the electrode, and despite this effect, would be: $\tau_r < 1/k_L a$ (Van't Riet, 1979; Johnson et al., 1990). These limitations have been widely described in the literature (Akita and Yoshida, 1973; Popovic and Robinson, 1989; Merchuk et al., 1990). When only one probe is used this method is difficult, because it strongly depends on the modelling of probe dynamics, on the position of the probe in the reactor, and on the assumption over hydrodynamic conditions. These effects can be more important in bubble columns (Gourich et al., 2008). The characteristic time of commercial fast oxygen electrochemical sensors, τ_r, ranges generally around 5 s. The dynamic of the electrode can be neglected only if the time for the oxygen transfer process ($1/k_L a$) is higher than 10 τ_r (≈50 s). When the probe response is not fast enough, which is currently the case in bubble columns (where 10 s < $1/k_L a$ < 100 s), oxygen concentration measurements correspond to a second-order process due to the probe influence. According to the work of Merchuk et al. (1990) mass transfer data analysis for dynamic $k_L a$ determination can be simplified by truncation of the first part of the electrode response curve and applying the first-order approximation; nevertheless, truncating more than 30% of the lower end data is not recommended. These results are consistent with those obtained by Gourich et al. (2008) for a modelling of mass transfer assuming a perfectly mixed flow with transient hydrodynamic effects.

3. Direct measuring of OTR in bioprocesses

3.1. Gas phase analysis

This method uses a gaseous oxygen analyzer to measure the oxygen concentration both in the inlet and the outlet gas stream of the bioreactor and a probe for measuring the dissolved oxygen concentration in the liquid. An oxygen mass balance under steady-state conditions yields:

$$F_{O_2}^{in} - F_{O_2}^{out} - V \cdot OUR = 0 \quad (22)$$

where OUR is the oxygen uptake rate, F^{in} and F^{out} the molar flow rates measured at bioreactor inlet and outlet, and V the bioreactor volume.

At steady-state, the rate of oxygen transfer from the bubbles is equal to the rate of oxygen consumption by the cells:

$$k_L a \cdot \left(C^* - C_L\right) = OUR \quad (23)$$

Once the oxygen uptake rate is determined from the measurement of oxygen in the exhaust gas and, at the same time, the dissolved oxygen concentration is measured in the medium, $k_L a$ can be calculated according to:

$$k_L a = \frac{F_{O_2}^{in} - F_{O_2}^{out}}{V \cdot \left(C^* - C_L\right)} \quad (24)$$

where C_L is the oxygen concentration in the liquid phase and C^* is the equilibrium or saturation concentration of the oxygen in the liquid under the temperature and pressure conditions in the bioreactor.

This technique is based on measuring the oxygen concentration of the air inflow and air outflow, accurate modelling of gas phase mixing being required for the correct interpretation of the measurement of the oxygen transfer rate (Van't Riet, 1979). Also, it is important to take into account the fraction of the oxygen consumed because, if oxygen uptake rate is low, the variation of the oxygen concentration between the inlet and the outlet of the gas stream is very small, and it becomes necessary to use very sensitive measuring equipment. On the other hand, if the size of the bioreactor is large, the variation in driving force $(C^* - C_L)$ in the bioreactor can be significant. In this case, the logarithmic average value between the inlet and outlet of the gas stream can be a good approximation for the driving force.

3.2. Dynamic methods

The dynamic methods are based on the technique proposed by Taguchi and Humphrey (1966), measuring the respiratory activity of microorganisms which are actively growing in the bioreactor. If the gas supply to the bioreactor is turned off, the dissolved oxygen concentration will decrease at a rate equal to oxygen consumption by the respiration of microorganism (Fig. 5). Under these conditions Eq. (5) can be simplified to:

$$\frac{dC_L}{dt} = -q_{O_2} \cdot C_X \quad (25)$$

obtaining OUR from the slope of the plot of dissolved oxygen concentration (after stopping air flow) *vs* time; biomass concentration must be known (or measured) at this time.

When the aeration is turned on again, the dissolved oxygen concentration increases until it reaches the steady oxygen concentration, and by using the estimated OUR value, $k_L a$ can be determined from the measured profile of dissolved oxygen concentration, using Eq. (5) again. Under these conditions, for a given biomass concentration, C_X, and once q_{O2} value is known, Eq. (5) can be integrated, taking into account the time at which the aeration

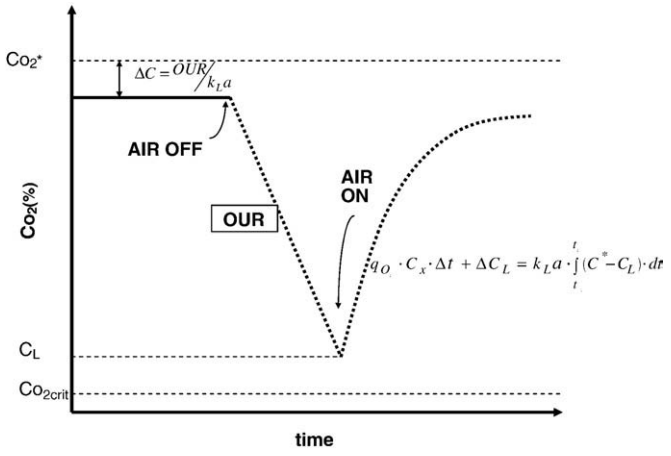

Fig. 5. Schematic description of the direct measuring of OTR in bioprocess by the classical dynamic technique.

of the culture is restored ($t = t_1 \therefore C = C_L$, known), and the following equation can be applied:

$$q_{O_2} \cdot C_X \cdot \Delta t + \Delta C_L = k_L a \cdot \int_{t_1}^{t_2} \left(C^* - C_L\right) \cdot dt \quad (26)$$

Eq. (26) can be used to determine the volumetric oxygen mass transfer several times during the production process, solving this equation for each data set of experimental values of C_L *vs.* time.This method is simple, and can be applied during an actual fermentation, when the response time of the oxygen electrode is lower than the characteristic time for the mass transfer processes, as commented above (Garcia-Ochoa et al., 2000a; Bandaiphet and Prasertsan, 2006; Djelal et al., 2006). However, this method is not applicable to situations in which OUR can not be determined correctly when the gas supply is turned off, e.g., when the dissolved oxygen concentration is very low. In this case a modified dynamic method can be used (Gomez et al., 2006). The modification consists in using a step change of air to pure oxygen in the inlet gas stream or *vice versa*. The evolution of dissolved oxygen concentration in the transition between two pseudo-steady states allows the OUR and $k_L a$ calculations. Oxygen concentration changes as the result of both physical oxygen absorption (or desorption) and oxygen consumption by microbial culture.

Assuming that q_{O2}, C_X, C^* and $k_L a$ are constant during the measurement time, Eq. (5) can be now expressed as:

$$\frac{dC}{dt} = c - k_L a \cdot C \quad (27)$$

where c is a constant given by:

$$c = k_L a \cdot C^* - q_{O_2} \cdot C_X \quad (28)$$

The integration of Eq. (27) when oxygen is absorbed with the boundary conditions:

$t = 0 \therefore C^* = C^*_0 \therefore C = C_{Lo}$ and $t = t_1 \therefore C = C_L$, yields the following equation:

$$C_L = \left(C_0^* - \frac{q_{O_2} \cdot C_X}{k_L a}\right) - \left(C_0^* - C_{L_0} - \frac{q_{O_2} \cdot C_X}{k_L a}\right) \cdot e^{-k_L a \cdot t} \quad (29)$$

and when oxygen is desorbed, with the following boundary conditions: $t = t_1 \therefore C^* = C^*_1 \therefore C = C_{L1}$, and $t = t_2 \therefore C = C_L$, the equation obtained results:

$$C_L = \left(C_1^* - \frac{q_{O_2} \cdot C_X}{k_L a}\right) + \left(C_{L_1} - C_1^* - \frac{q_{O_2} \cdot C_X}{k_L a}\right) \cdot e^{-k_L a \cdot t} \quad (30)$$

Eqs. (29) and (30) represent, respectively, the evolution of oxygen concentration in the liquid phase (C_L) when the composition of the gas stream is modified changing air to pure oxygen or, if previously saturated with pure oxygen, when the gas stream is changed to air. Fig. 6 is a typical representation of the results obtained during an experiment using dynamic absorption or desorption of pure oxygen for k_La and OUR determination.

3.3. Other methods

Other techniques have been proposed for measuring the volumetric mass transfer coefficient, which improve some aspects of the classical methods. Some of them are based on a chemical reaction, like hydrazine oxidation (Onken et al., 1985), bio-oxidation of catechol forming 2-hydroxymuconic semialdehyde catalyzed by the enzyme catechol-2,3-dioxygenase (Ortiz-Ochoa et al., 2005), another uses the change of pH by constant bubbling of carbon dioxide into a well-mixed reactor (Hill, 2006). Other methods consist in the measurement of the oxygen limited growth rate of a strictly aerobic microorganism (Duetz et al., 2000).

There are also techniques for mass transfer coefficient determination based on physical methods (Mignone, 1990; Gauthier et al., 1991; Linek et al., 1994; Carbajal and Tecante, 2004), or by absorption of some compound such as the krypton method (Pedersen et al., 1994), which is based in the injection of Kr-85 (volatile radio-isotope that emits beta and gamma radiation) into the medium and the measurement of the radioactivity in the outlet gas stream.

3.4. Comparison of the k_La values obtained by different methods

As pointed out above, chemical methods have the limitation of the changes in fluid dynamics caused by the addition of chemicals. Among physical methods, the dynamic method is by far the most commonly used in the last decades to evaluate k_La, due to its simplicity and relative accuracy. Both the absorption and desorption measurements give equal values of k_La under identical hydrodynamics conditions (Gomez, 1995; Sanchez et al., 2000) although, if the characteristic time for oxygen electrode is of the same magnitude as the characteristic time for the oxygen transfer process ($1/k_La$), the dynamic response of the electrode must be taken into account for determining correct values of k_La.

In Fig. 7, as an example, k_La values obtained by different methods as a function of stirrer speed in non-Newtonian solutions and 20 L vessel are compared ($V_S = 2\cdot10^{-3}$ m·s^{-1} and $\mu_a = 8\cdot10^{-3}$ to $30\cdot10^{-3}$ Pa·s). The k_La values obtained by Ogut and Hatch (1988), using the sulfite measurement method, are much higher than those usually obtained for an electrolyte solution. The difference is greater for lower values of

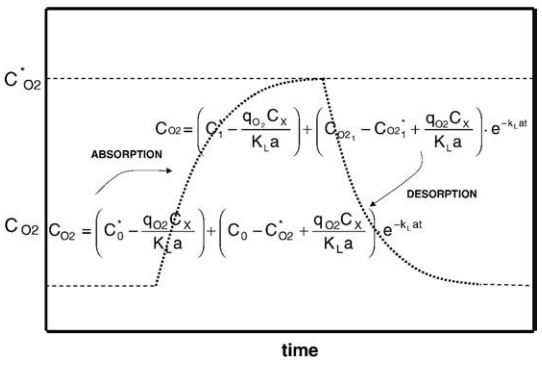

Fig. 6. Evolution of oxygen concentration in the liquid-phase when the composition of the gas stream is modified changing from air to pure oxygen (absorption) or from pure oxygen to air (desorption).

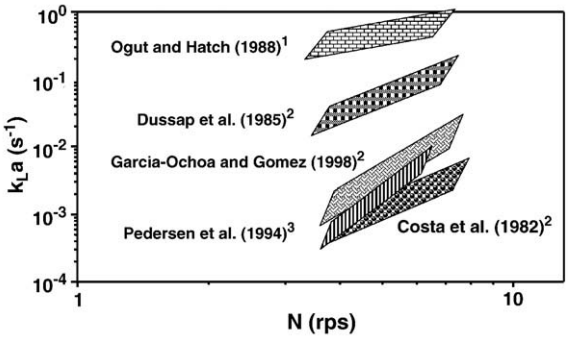

Fig. 7. Comparison of k_La values obtained by different measuring methods as a function of stirrer speed in non-Newtonian solutions. Key: 1: chemical method, 2: dynamic method, 3: Kr measurement (adapted from Garcia-Ochoa and Gomez, 1998).

stirrer speed. This is due in part to the strong ionic state of the sulfite solution and in part to the chemical reaction enhancement of transfer rate (Thibault et al., 1990). The difference between the results obtained by other authors can be explained by the effect of certain distinctive features in the reactor used (like D/T ratio, stirrer and sparger type, etc.) on the k_La values. In Table 1 a comparison of different methods for volumetric mass transfer coefficient determination in bioprocesses is shown.

4. Empirical correlation of k_La values

In the literature, both dimensional and dimensionless equations for the volumetric mass transfer coefficient as a function of different variables have been proposed. However, there are considerable problems concerning the accuracy of k_La estimation, and frequent discrepancies between experimental data and those estimated from these equations are found, mainly when k_La for real broths are estimated from equations proposed for aqueous solutions. This can be due to the strong influence of the type and size of the bioreactor, the different range of operational conditions, the system considered — solutions or real broths, the influence of physicochemical properties on hydrodynamics due to high viscosity of the liquid, its rheological behavior or even the measuring method used (Gogate et al., 2000; Garcia-Ochoa and Gomez, 1998).

The volumetric mass transfer coefficient increases significantly when ion concentration in the solution is raised. The addition of electrolyte increases gas hold-up, due to its influence on decreasing bubble size and the non-coalescence effect at both low and high pressures (Wilkinson et al., 1994; Gogate et al., 2000; Puthli et al., 2005). According to Van't Riet (1979), k_La for ionic solutions are more depending on P/V than those for pure water. The k_La values decrease with increasing liquid viscosity (Garcia-Ochoa and Gomez, 1998; Garcia-Ochoa et al., 2000a; Kilonzo and Margaritis, 2004) and increase with temperature (Hiraoka et al., 2001). The addition of surfactants or antifoams, substances commonly added to culture medium, provokes a high decrease of k_La values, compared to those of pure water (Kawase et al., 1992a, Garcia-Ochoa and Gomez, 2005). This can be due to the effect of surfactant molecules affecting the hydrodynamic parameters: the average bubble size may increase due to induced bubble coalescence which, in turn, will affect the gas hold-up, hence, the mass transfer area (Arjunwadkar et al., 1998). Other authors have pointed out the barrier effect of these substances, due to a mono-layer of the surfactants formed at the interface, which can offer resistance to crossing by the gas molecules (Yagi and Yoshida, 1974; Van der Meer et al., 1992; Vasconcelos et al., 2003; Dai et al., 2004; Linek et al., 2005). Some of these works showed that the addition of active-surface compounds induced a significant reduction on the mass transfer

Table 1
Comparison of different methods for volumetric mass transfer coefficient evaluation

Method	$k_La \cdot 10^2$ Range (s^{-1})	Assay time	Scale applied	Assumptions / drawback	References
Sodium sulphite	0 to 0.3	Hours	Lab scale	Alteration of driving force, diffusion coefficient and coalescence properties; complex kinetics boundary layer reduction. Can not be applied to microbial processes	Cooper et al. (1944)
Absorption of Carbon dioxide	0 to 0.1	Minutes	Lab scale	Alteration driving force. Change of the coalescence behaviour. Can not be applied to microbial processes	Danckwerts and Gillham (1966)
Gas phase analysis	0 to 0.3	Minutes	>100 mL	Invasive probes are necessary; only possible during active oxygen consumption; requires large gas flows and gas analysis. The accuracy depend on precision of oxygen analyzer	Wang et al. (1979)
Dynamic: Desorption or absorption oxygen	0 to 0.1	Minutes	>100 mL	Invasive probes are necessary. High oxygen dissolved concentration are necessary. Probe response time must be considered; gassing time can be significant at larger scales. Dynamic changes in dissolved oxygen may disturb the microbial metabolism	Taguchi and Humphrey (1966)
Growth of strict aerobic microorganism	0.06 to 0.1	Hours	Any scale	Assumptions about growth kinetics are required; experimentally laborious	Duetz et al. (2000)
Hydrazine oxidation	0 to 0.5	Minutes	Semi-industrial scale	Homogeneous oxidation of hydrazine. Hydrazine does not accumulate. No chemical enhancement	Onken et al. (1985)
Bio-oxidation of catechol	<0.1	Minutes	<100 mL	Available of oxidative enzyme; limited to small scale	Ortiz-Ochoa et al. (2005)
Kr Method	0 to 0.3	Minutes	Any scale	The use of isotope radioactive may cause some problems in an industrial application. Can be applied to microbial processes	Pedersen et al. (1994)
Measurement pH for CO_2 solutions	0 to 0.1	Minutes	Any scale	Salt addition does not improve the mass transfer rate of CO_2. Can not be applied to microbial processes	Hill (2006)

coefficient, between 80 and 40% depending on the surface tension value.

On the other hand, improvement of OTR by addition of hydrocarbons has been reported by Dumon and Delmas (2003) and Clarke et al. (2006); these latter authors found that k_La is enhanced with increasing alkane concentration between 0 and 10%. For this variation several possible causes have been suggested: the alkane spreads as a thin film on the bubble and acts by decreasing the surface tension and increasing the interfacial area; the drops act as rigid spheres thereby increasing turbulence; the drops modify the medium so that it can carry more oxygen; or maybe a reduction in gas bubble diameter is the effect provoked.

Thus, in hydrocarbon-aqueous dispersions, the hydrocarbon impacts markedly on k_La, but in widely differing manners depending on the hydrocarbon type and concentration, the process conditions and the geometric constraints under consideration. This gives rise to three distinct k_La behavioural trends with an increase in hydrocarbon concentration: k_La increase to a maximum, with subsequent decease; k_La increase to a maximum with no decrease and no increase in k_La or k_La decrease (Clarke and Correia, 2008).

4.1. Stirred tank bioreactors

In mechanical agitated bioreactors, the stirrer is the main gas-dispersing tool and stirrer speed and design have both a pronounced effect on mass transfer. Empirical correlations for the volumetric mass transfer coefficient depend on several geometrical parameters, although there is no agreement in the literature about how to take into account this influence. Van't Riet (1979) proposed a correlation of k_La with P/V, stating that there is no influence of stirrer geometry and the number of stirrers on mass transfer in non-viscous systems. However, Zhu et al. (2001) were able to increase the mass-transfer rate by 17% by changing the impeller, and Puthli et al. (2005) found that k_La values are affected by the stirrer configuration.

Table 2
Exponent values in Eq. (31) for stirred tank bioreactors

Autors	System	N	P/V	V_s	μ_a	Volume (L)	Stirrer Type
Yagi and Yoshida (1975)	Water + glycerol	2.2	0.8	0.3	−0.4	12	6FBT
	CMC / PANa		0.8	0.3			
Figueiredo and Calderbank (1979)	Water	–	0.6	0.8	–	600	FBT
Van't Riet (1979)	Water	–	0.4	0.5	–	2–2600	Any
Nishikawa et al. (1981)	Water Millet /CMC	2.4	0.8	0.33	−0.5	2.7–170	FBT & FBP
		2.4					
Chandrasekharan and Calderbank (1981)	Water	–	0.55	$0.55 \cdot D^{-1/2}$		50–1430	FBT
Davies et al. (1985)			0.8	0.45		20–180	6FBT
Kawase and Moo-Young (1988)			1.0	0.5			
Ogut and Hatch (1988)		0.9		0.7		100	6FBP
		0.5		0.5	−0.4		
Linek et al. (1991)	Water		0.65	0.4		20	6FBT
			1.1				
Pedersen et al. (1994)	Water+xanthan	2.7	–	0.5–0.7	–	15	Two-6FBT
Gagnon et al. (1998)			0.6–0.8	0.5		22	6FBT
Arjunwadkar et al. (1998)	Water + electrolytes / CMC		0.68	0.4–0.58		5	FBT & PBT
Vasconcelos et al. (2000)	Water		0.62	0.49		5	Two-6FBT
Garcia-Ochoa and Gomez (1998, 2001)	Water/Water+xanthan	2.0	0.6	0.5–0.67	−0.67	2–25	1,2-FBT, CBT, FBP,
					−1*		CBP, PBP
Puthli et al. (2005)	Water+electrolytes./CMC		0.57–0.98	0.53	−0.84	2	1,2-FBT, FBP, PBP

* Casson viscosity model.
Acronyms for Stirrers on Table 2: CBT: Curved Blade Turbine. CBP: Curved Blade Paddle. FBP: Flat Blade Paddle. FBT: Flat Blade Turbine. PBP: Pitched Blade Paddle. PBT: Pitched Blade Turbine. Two-6FBT: Two stirrers of the type indicated (6FBT, in the example).

The k_La values have also been correlated with the combination of stirrer speed, N, superficial gas velocity, V_S, and liquid effective viscosity, μ_a, obtaining equations such as the following:

$$k_La = C \cdot V_s^a \cdot (P/V)^b \cdot \mu_a^c \quad (31)$$

where the constant C depends on the geometrical parameters of the vessel and the stirrer employed. Other equations proposed substitute the average power input per volume, P/V, by the effect of stirrer speed, N. Table 2 gives the values of the exponents of different correlations available in the literature. It can be seen that the exponent values (a, b and c) show a wide variation range in the different correlations proposed by different authors: $0.3 \le a \le 0.7$; $0.4 \le b \le 1$; $-0.4 \le c \le -0.7$. For non-viscous systems the most frequently used correlation is that from Van't Riet (1979).

Another approach is to use equations with dimensionless groups. k_La is included in Sherwood (k_LaT^2/D_L) o Stanton (k_LaV/Q) numbers, expressed as a function of different dimensionless numbers such as Reynolds ($\rho NT^2/\mu_a$), Schmidt ($\mu_a/\rho D_L$), Weber ($\rho N^2T^3/\sigma$), Aeration (NT/V_S), Froude (N^2T/g), geometrical parameters of the bioreactor and rheological properties of the fluid. Table 3 and 4 show some of the dimensionless correlations available in the literature for Newtonian and non-Newtonian fluids. These can be divided into those which reflect the effect of the stirrer speed directly (N) and those which take into account the power input (P). The correlation of Nishikawa et al. (1981) is the only one to include both variables. Yagi and Yoshida (1975) used various liquids and gases to deduce the equations proposed, although no effect of gas viscosity, as implied in the equation of Perez and Sandall (1974), could be observed. In addition, these authors take into account the effect of viscoelasticity in the form of the Deborah number (λN), but the method for evaluation of characteristic material time (λ) from the shear rate depending on the apparent viscosity can be applied only to liquids approaching Newtonian flow behavior (Herbst et al., 1992). Nishikawa et al. (1981) differentiated between mass transfer resulting from stirred and from bubbling systems, although the latter contribution is usually negligible. The relationships proposed by Höcker et al. (1981) and Schlüter and Deckwer (1992) are the only approach considering the gas flow rate rather than superficial gas velocity; and that proposed by Albal et al. (1983) is unrealistic because the influence of gas flow is not considered. In the presence of biotransformation similar equations have been proposed and values for these exponents have been reported (Pedersen et al., 1994; Garcia-Ochoa et al., 2000a).

4.2. Bubble columns and airlift bioreactors

Bubble columns and airlift bioreactors are the two main types of pneumatically agitated reactors. However, much more information exists on gas–liquid mass transfer in conventional bubble columns than in airlift bioreactors. Encyclopedias, books or chapter of books (Merchuk, 1986; Chisti, 1989; Schügerl and Lübbert, 1995; Merchuk and Gluz, 1999), several reviews (Chisti, 1998; Kilonzo and Margaritis, 2004; Kantarci et al., 2005) and many papers (Suh et al., 1991; Wilkinson et al., 1994; Li et al., 1995; Eickenbusch et al., 1995; Al-Masry and Abasaeed, 1998; Sanchez et al., 2000; Vasconcelos et al., 2003) deal with these reactor types.

Table 3
Dimensionless correlations for prediction of k_La in Newtonian fluids in stirred tanks

Authors	Dimensionless equation
Perez and Sandall (1974)	$\frac{k_LaT^2}{D_L} = 21.2 \cdot \left(\frac{\rho NT^2}{\mu_a}\right)^{1.11} \cdot \left(\frac{\mu_a}{\rho D_L}\right)^{0.5} \cdot \left(\frac{V_sT}{\sigma}\right)^{0.45} \cdot \left(\frac{\mu_c}{\mu_a}\right)^{0.69}$
Yagi and Yoshida (1975)	$\frac{k_LaT^2}{D_L} = 0.06 \cdot \left(\frac{\mu_a}{\rho D_L}\right)^{0.5} \cdot \left(\frac{T^2N\rho}{\mu_a}\right)^{1.5} \cdot \left(\frac{\mu_aV_s}{\sigma}\right)^{0.6} \cdot \left(\frac{N^2T}{g}\right)^{0.19} \cdot \left(\frac{NT}{V_s}\right)^{0.32}$
Nishikawa et al. (1981)	$\frac{k_LaD^2}{D_L} = 0.368 \cdot \left(\frac{\rho NT^2}{\mu}\right)^{1.38} \cdot \left(\frac{\mu}{\rho D_L}\right)^{0.5} \cdot \left(\frac{\mu V_s}{\sigma}\right)^{0.5} \left(\frac{N^2T}{g}\right)^{0.367} \cdot \left(\frac{NT}{V_s}\right)^{0.167} \cdot \left(\frac{T}{D}\right)^{0.25} \cdot \left(\frac{P/V}{\rho N^3T^5}\right)^{0.75}$
Costa et al. (1982)	$\frac{k_LaT^2}{D_L} = 8.38 \cdot \left(\frac{\rho N^{2-n}T^2}{k}\right)^{2/3} \cdot \left(\frac{k}{\rho N^{1-n}D_L}\right)^{1/3} \cdot \left(\frac{\rho N^2T^3}{\sigma}\right)^{0.43} \left[1 + 1.5 \cdot 10^{-3} \cdot \left(\frac{\rho N^2T^3}{\sigma}\right)\right] \cdot \left(\frac{NT}{V_s}\right)^{-0.4} \cdot \left(\frac{T}{D}\right)$
Albal et al. (1983)	$\frac{k_LaT^2}{D_L} = 1.41 \cdot 10^{-3} \cdot \left(\frac{\mu_a}{\rho D_L}\right)^{0.5} \cdot \left(\frac{T^2N\rho}{\mu_a}\right)^{0.67} \cdot \left(\frac{\rho N^2T^3}{\sigma}\right)^{1.29}$
Schlüter and Deckwer (1992)	$k_La\left(\frac{\nu}{g^2}\right)^{1/3} = C \cdot \left[\frac{P/V}{\rho(\nu g^4)^{1/3}}\right]^{0.62} \cdot \left[\frac{Q}{V} \cdot \left(\frac{\nu}{g^2}\right)^{1/3}\right]^{0.23}$

Table 4
Dimensionless correlations for prediction of k_La in non-Newtonian fluids in stirred tanks

Authors	Dimensionless Equation
Yagi and Yoshida (1975)	$\frac{k_LaT^2}{D_L} = 0.06 \cdot \left(\frac{\rho NT^2}{\mu_a}\right)^{1.5} \cdot \left(\frac{N^2T}{g}\right)^{0.19} \cdot \left(\frac{\mu_a}{\rho D_L}\right)^{0.5} \cdot \left(\frac{NT}{V_s}\right)^{0.32} \left(\frac{\mu_aV_s}{\sigma}\right)^{0.6} \cdot \left[1 + 2(\lambda N)^{0.5}\right]^{-0.67}$
Nishikawa et al. (1981)	$\frac{k_LaD^2}{D_L} = 0.115 \cdot \left(\frac{T^2N\rho}{\mu_a}\right)^{1.5} \cdot \left(\frac{\mu_a}{\rho D_L}\right)^{0.5} \cdot \left(\frac{\mu_aV_s}{\sigma}\right)^{0.5} \cdot \left(\frac{TN^2}{g}\right)^{0.37} \left(\frac{NT}{V_s}\right)^{0.17} \cdot \left(\frac{D}{T}\right)^2 \cdot \left(\frac{P_0}{N^3T^5\rho}\right)^{0.8} \cdot \left[1 + 2(\lambda N)^{0.5}\right]^{-0.67} + + 0.112 \cdot \left(\frac{P/V}{N^3T^5\rho + P/V}\right) \cdot \left(\frac{V_s}{(gD)^{0.5}}\right) \cdot \left(\frac{k(CV_s)^{n-1}}{\rho D_L}\right)^{0.5} \cdot \left(\frac{gD^2\rho}{\sigma}\right)^{0.66} \left(\frac{gD^3\rho^2}{\left[k(CV_s)^{n-1}\right]^2}\right)^{0.42} \cdot \left[1 + 0.18\left(\lambda\frac{v_b}{d_b}\right)^{0.45}\right]^{-1}$
Höcker et al. (1981)	$\frac{k_LaV}{Q} = 0.105 \cdot \left(\frac{P}{Q\rho^{1/3}g^{1/3}a_a/\rho^{2/3}}\right)^{0.59} \cdot \left(\frac{\mu_a}{\rho D_L}\right)^{-0.3}$
Garcia-Ochoa and Gomez (1998)	$\frac{k_LaT^2}{D_L} = 6.86 \cdot \left(\frac{\rho N^{2-n}T^2}{kN^{n-1}}\right)^{2/3} \cdot \left(\frac{NT}{V_s}\right)^{-2/3} \cdot \left(\frac{\rho N^2T^3}{\sigma}\right)^1$ $\frac{k_LaT^2}{D_L} = 0.022 \cdot \left(\frac{\rho NT^2}{\mu_c}\right)^1 \cdot \left(\frac{NT}{V_s}\right)^{-2/3} \cdot \left(\frac{\rho N^2T^3}{\sigma}\right)^1$

Kilonzo and Margaritis (2004) have reviewed the effects of non-Newtonian fermentation broth viscosities on gas–liquid mixing and oxygen mass transfer characteristics in airlift bioreactors. Also, Letzel et al. (1999) reported an increase of k_La with increasing pressure caused by the increase in total gas hold-up; although, once a limit for non-coalescence concentration has been reached, the increase is much smaller. Moreover, with large reactors, the hydrostatic pressure can be assumed to have an effect on k_La (Znad et al., 2004).

As in stirred tanks bioreactors, many empirical equations have been proposed to estimate k_La values in bubble columns and airlift reactors. Dimensional equations establish relationships between k_La and superficial gas velocity, the properties of the fluid and the geometric factors of bioreactor (height of the column, diameter of the column and sparger characteristics, mainly), although these last ones have relatively little influence. Thus, the volumetric mass transfer coefficient is expressed by dimensional equations generally in the form:

$$k_La = C \cdot V_s^a \cdot \mu_a^b \quad (32)$$

For classical bubble columns and using pure water, Deckwer et al. (1974, 1983) determined values of the constant, C, and of the exponent, a, of 0.47 and 0.82, respectively. In saline solutions they propose for the constant C values between 0.12 and 9.5 and for the exponent, a, between 0.72 and 1.28. For non-Newtonian fluids the apparent viscosity is introduced in the equations and the exponent b takes a value between −0.8 and −1 (Godbole et al., 1984).

For internal loop airlift reactor, ascending flow by the circular and descendent crown by the central zone, Halard et al. (1989) have verified that the equation proposed by Godbole et al. (1984), for classic bubble columns, can be used for non-Newtonian fluids.

In the case of external loop airlift reactor, expressions based on the ratio of down-comer to riser cross sectional area (A_D/A_R), the effective viscosity of the dissolution and other fluid-dynamic parameters have been proposed (Bello et al., 1984; Popovic and Robinson, 1989):

$$k_La = C \cdot V_s^a \mu_a^b \cdot \left(1 + \frac{A_D}{A_R}\right)^c \cdot V_{LR}^d \cdot \phi^e \quad (33)$$

Table 5 shows some of the values of the exponents of these correlations available in the literature for Newtonian and non-

Table 5
Exponent values in Eq. (33) for bubble columns and airlifts

Authors	System	Vs	$1+A_D/A_R$	V_{LR}	ϕ	μ_a
Deckwer et al. (1974, 1983)	Water Water+ electrolytes	0.7–1.3				
Jackson and Shen (1978)	Water	1.2				
Bello et al. (1984)	Water/Water+ electrolytes	0.9	−1	0.1		
Godbole et al. (1984)	CMC	0.44–0.59				−0.8 to −1
Popovic and Robinson (1989)	CMC	0.52	−0.85			−0.89
Li et al. (1995)	Non-Newtonian	0.52				−0.26
Al-Masry and Abasaeed (1998)	Newtonian	0.76	−2.41			−0.76
Sanchez et al. (2000)	Tap and sea water	0.94–1.17			1	

Newtonian fluids. As can be seen the exponent of $(1+A_D/A_R)$ is negative and therefore a decrease in k_La is predicted with increasing down-comer to riser cross sectional area ratio (A_D/A_R). The (A_D/A_R) ratio is a key design parameter, which controls the hydrodynamics of the system, and thus also the oxygen transfer rate in airlift reactors. Furthermore, the correlations of Popovic and Robinson (1989) and Li et al. (1995) include a problematic definition of the apparent viscosity, defining shear rate as a linear function of the gas velocity. This approach can be questionable from a rheological point of view because it will predict the same shear rate for a certain superficial gas velocity, no matter which liquid is used (Kawase and Hashiguchi, 1996; Chisti, 1998).

In the same way as in stirred tanks, the equations based on dimensionless numbers predict the k_La coefficient, included on number of Sherwood (k_LaD^2/D_L), as a function of other dimensionless numbers: Schmidt ($\mu/D_L\rho$), Bondenstein ($gD^2\rho/\sigma$), Galileo ($gD^3\rho^2/\mu^2$), Froude (V_S/gD), Deborah ($\lambda V_S(1+\varepsilon)/\varepsilon d_b$) and Weissenberg ($N_c/\tau$). Different equations proposed are given in Table 6; among these equations, that from Akita and Yoshida (1973) is the most amply used, although it is limited to bubble columns with diameter less to 0.6 m and a simple gas sparger. The equation proposed by Suh et al. (1991) has been employed successfully by these authors to correlate k_La values in the production of the extracellular polysaccharide xanthan by *Xanthomonas campestris* in bubble columns and air-lifts (Suh et al., 1992); however the apparent viscosity was calculated assuming the shear rate to be equal to $2800{\cdot}V_S$. It should be emphasized that the validity and application of these correlations depend very much on the measurements of the flow behavior of the liquid and also on the assumption regarding the estimation of a representative shear rate for predicting the apparent viscosity. The value of k_La determined for a microbial system can differ substantially from those obtained for oxygen absorption in water or in simple aqueous solutions, i.e., in static systems with an invariable composition of the liquid media along the time. Hence k_La values should be determined in the biosuspension, which involve the actual media and microbial population.

5. Prediction of oxygen transfer rate

Although a large amount of experimental data and a number of equations to predict oxygen mass transfer rate are available, it should also be stressed that none of the overall correlations for k_La have universal applicability. Therefore, to further explain the gas–liquid mass transfer phenomena, it is important to know the influence of hydrodynamic factors on k_L and a, independently.

5.1. Mass transfer coefficient prediction

The mass transfer coefficient k_L in bioreactors can be estimated by a large number of equations (Table 7). Most of them are empirical (Johnson and Huang, 1956; Calderbank and Moo-Young, 1961; Perez and Sandall, 1974) and others have a theoretical base (Prasher and Wills, 1973; Kawase et al., 1987; Kawase et al., 1992a; Zhang and Thomas, 1996). The theoretical models to predict the mass transfer coefficient are divided according to different approaches. Some of them are based on the concept of a rigid interface (Whitman, 1923), others in an interface where surface renewal occurs through the displacement of liquid at the interface (Higbie, 1935; Danckwerts, 1951; Lamont and Scott, 1970) or a combination of those concepts (Toor and Marchelo, 1958). These models are summarized in Table 8.

Higbie's penetration theory is widely accepted for gas–liquid transfer description (Kawase et al., 1987; Tobajas et al., 1999; Garcia-Ochoa and Gomez, 2005; Billet and Schultes, 1993; Kawase and Hashiguchi, 1996; Shimizu et al., 2000, 2001). The physical concept behind the penetration theory is that there is a continual attachment and detachment of small liquid eddies at the gas–liquid interface; in the interval of attachment, there is an interchange of solute by molecular diffusion. When a gas bubble moves through a liquid it continually creates new interfacial area at its advancing tip and, assuming a non-stationary diffusion of the liquid elements in the gas–

Table 6
Dimensionless correlations for prediction of k_La in bubble columns and air-lifts in Newtonian and non-Newtonian fluids

Authors	Dimensionless Equation
Akita and Yoshida (1973)	$\frac{k_LaD^2}{D_L}=0.6\cdot\left(\frac{D^2\rho g}{\sigma}\right)^{0.62}\cdot\left(\frac{D^3\rho^2 g}{\mu^2}\right)^{0.3}\cdot\left(\frac{\mu}{\rho D_L}\right)^{0.5}\cdot\phi^{1.1}$
Nakanoh and Yoshida (1980)	$\frac{k_LaD^2}{D_L}=0.09\cdot\left(\frac{D^2\rho g}{\sigma}\right)^{0.75}\cdot\left(\frac{D^3\rho^2 g}{\mu^2}\right)^{0.4}\cdot\left(\frac{\mu}{\rho D_L}\right)^{0.5}\cdot\left(\frac{V_S}{\sqrt{gD}}\right)^{1}$
	$\frac{k_LaD^2}{D_L}=0.09\cdot\left(\frac{D^2\rho g}{\sigma}\right)^{0.75}\cdot\left(\frac{D^3\rho^2 g}{\mu^2}\right)^{0.4}\cdot\left(\frac{\mu}{\rho D_L}\right)^{0.5}\cdot\left(\frac{V_S}{\sqrt{gD}}\right)^{1}\cdot\left[1+0.13\left(\frac{\lambda V_S(1-\phi)}{\phi\cdot d_b}\right)^{0.55}\right]$
Kawase et al. (1987)	$\frac{k_LaD^2}{D_L}=0.452\cdot\left(\frac{D^2\rho g}{\sigma}\right)^{0.6}\cdot\left(\frac{V_S}{\sqrt{gD}}\right)^{0.3}\cdot\left(\frac{\mu}{\rho D_L}\right)^{0.5}\cdot\left(\frac{DV_S}{\nu_L}\right)$
Uchida et al. (1989)	$\frac{k_LaD^2}{D_L}=0.17\cdot\left(\frac{D^2\rho g}{\sigma}\right)^{0.62}\cdot\left(\frac{D^3\rho^2 g}{\mu^2}\right)^{0.3}\cdot\left(\frac{\mu}{\rho D_L}\right)^{0.5}\cdot\phi^{1.1}$
Vatai and Tekic (1989)	$\frac{k_LaD^2}{D_L}=0.031\cdot\left(\frac{D^2\rho g}{\sigma}\right)^{0.75}\cdot\left(\frac{D^3\rho^2 g}{\mu^2}\right)^{0.4}\cdot\left(\frac{\mu}{\rho D_L}\right)^{0.5}\cdot\left(\frac{V_S}{\sqrt{gD}}\right)^{1}$
Suh et al. (1991)	$\frac{k_LaD^2}{D_L}=0.018\left(\frac{\mu}{\rho D_L}\right)^{0.5}\left(\frac{D^2\rho g}{\sigma}\right)^{0.2}\left(\frac{gD^3\rho^2}{\mu^2}\right)^{0.62}\left(\frac{V_S}{gD}\right)^{0.5}\left[\frac{1}{1+0.12(N_l/\tau)}\right]$

Table 7
Equations proposed for mass transfer coefficient prediction

Author	Mass transfer coefficient
Johnson and Huang (1956)	$\frac{k_L\cdot D}{D_L}=0.0924\cdot\left(\frac{\nu}{D_L}\right)^{1/2}\cdot\left(\frac{N.T^2}{\nu}\right)^{0.71}$
Calderbank and Moo-Young (1961)	$\frac{k_L\cdot D_p}{D_L}=C\cdot\left(\frac{\mu}{\rho D_L}\right)^{1/3}\cdot\left(\frac{\varepsilon^{1/6}\cdot D_p^{2/3}}{\nu^{1/2}}\right)^{2/3}$
Lamont and Scott (1970)	$k_L=0.4\cdot\left(\frac{P/V}{\rho}\right)^{1/4}\cdot\left(\frac{D_L}{\nu}\right)^{1/2}$
Prasher and Wills (1973)	$k_L=C\cdot\left(\frac{\nu}{D_L}\right)^{-1/2}\cdot(\varepsilon\cdot\nu)^{1/4}$
Perez and Sandall (1974)	$\frac{k_L\cdot T}{D_L}=21.2\cdot\left(\frac{T^2N\rho}{\mu}\right)^{1.11}\cdot\left(\frac{\nu}{D_L}\right)^{1/2}\cdot\left(\frac{TV_S}{\sigma}\right)^{0.447}\cdot\left(\frac{\mu_c}{\mu}\right)^{0.694}$
Kawase and Moo-Young (1990)	$k_L=0.301\cdot(\varepsilon\cdot\nu)^{1/4}\cdot\left(\frac{\mu}{\rho D_L}\right)^{-1/2}$
Kawase et al. (1992a)	$k_L=\frac{4}{\sqrt{\pi}}\cdot 2^{\frac{1}{n}}\cdot\left(\frac{1}{T^*}\right)\sqrt{D_L}\left(\frac{\varepsilon\rho}{K}\right)^{\frac{1}{2(1+n)}}$
Zhang and Thomas (1996)	$k_L=C\cdot D^{1/2}\cdot\nu^{-1/4}\cdot\varepsilon^{1/4}$
Garcia-Ochoa and Gomez (2004)	$k_L=\frac{2}{\sqrt{\pi}}\cdot\sqrt{D_L}\left(\frac{\varepsilon\rho}{k}\right)^{\frac{1}{2(1+n)}};k_L=\frac{2}{\sqrt{\pi}}\cdot\sqrt{D_L}\left(\frac{\varepsilon\left(1-\sqrt{\alpha}\right)^2\rho}{\mu_c/\rho}\right)^{\frac{1}{4}}$
Linek et al. (2005)	$k_L=0.448\cdot\left(\frac{P/V}{\rho}\right)^{1/4}\cdot\left(\frac{D_L}{\nu}\right)^{1/2}$

Table 8
Definition of k_L in the different models of mass transfer

Author	Model	Mass Transfer Coefficient	Time dependence	Boundary Conditions
Whitman (1923)	Film	$k_L = \frac{D}{z_L}$	No	$z=0 \therefore C=C_i$ $z=z_L \therefore C=C_L \therefore$
Higbie (1935)	Penetration	$k_L = 2 \cdot \sqrt{\frac{D}{\pi \cdot t_e}}$	Constant	$z=0;\ t=0$ $\therefore C=C_L$ $0<t<te$ $\therefore C=C_i$ $z=\infty;\ 0<t<te$ $\therefore C=C_L$
Danckwerts (1951)	Surface removal	$k_L = \sqrt{D \cdot s}$	Functional	$z=0;\ t=0$ $\therefore C=C_L$ $0<t<\infty \therefore C=C_i$ $z=\infty;\ 0<t<\infty$ $\therefore C=C_L$
Toor and Marchelo (1958)	Film-penetration	$k_L = 2\sqrt{\frac{D}{\pi \cdot t_e}}\left(1+2\sqrt{\pi}\cdot\frac{z_L}{\sqrt{Dt_e}}\right)$ $k_L = \sqrt{Ds}\left[1+2\exp\left(-2z_L\sqrt{\frac{s}{D}}\right)\right]$	Functional	$te=0 \therefore C=C_L$ $z=0;\ 0<te<\infty$ $\therefore C=C_i$ $z=z_L;\ 0<te<\infty$ $\therefore C=C_L$

liquid interface during a contact or exposure time for mass transfer, t_e, the following equation can be obtained:

$$k_L = 2 \cdot \sqrt{\frac{D_L}{\pi \cdot t_e}} \tag{34}$$

It has been determined that k_L depends on the turbulence intensity, expressed as a function of the dissipated energy (Lamont and Scott, 1970; Prasher and Wills, 1973), while the surface renewal rate is considerably higher than that found for bubbles in free rise under potential flow (Figueiredo and Calderbank, 1979). Consequently, the experimental results would show that the exposure time is necessarily affected by eddies or turbulence at a microscopic scale. Therefore, the rate of dissipation of energy in the liquid per mass unit, ε, is the most adequate magnitude to characterize the time scale. The exposure time, t_e, that characterizes the residence time of micro-eddies at the interface, is generally unknown, but can be estimated by an adequate model. The evaluation of that time can be realized according to the Kolmogoroff's theory of isotropic turbulence, as the ratio of two characteristic parameters of eddies, namely, the eddy length, η, and the fluctuation velocity, u. Both parameters depend on the rate of dissipation of energy per mass unit, ε, and the cinematic viscosity, ν, according to:

$$\eta = \left(\frac{\nu^3}{\varepsilon}\right)^{\frac{1}{4}} \tag{35}$$

$$u = (\nu \cdot \varepsilon)^{\frac{1}{4}} \tag{36}$$

The exposure time is usually taken as the time that the bubbles take to travel a length equal to its diameter, and it is estimated using the ratio between eddy length and the fluctuation velocity of Kolgomoroff. This ratio for calculation of the exposure time value has been previously used in some works for the prediction of the volumetric mass transfer coefficient in bubble columns and external loop airlifts (Kawase et al., 1987; Kawase and Hashiguchi, 1996).

If the rheological model of Ostwald-de Waele is considered for description of non-Newtonian flow behaviour of fluids, the following equation is obtained (Kawase et al., 1987; Garcia-Ochoa and Gomez, 2005):

$$k_L = \frac{2}{\sqrt{\pi}} \cdot \sqrt{D_L}\left(\frac{\varepsilon \cdot \rho}{k}\right)^{\frac{1}{2\cdot(1+n)}} \tag{37}$$

while if the Casson model is used, the equation obtained is:

$$k_L = \frac{2}{\sqrt{\pi}} \cdot \sqrt{D_L}\left(\frac{\varepsilon \cdot \rho \cdot (1-\sqrt{\alpha_r})^2}{\mu_c}\right)^{\frac{1}{4}} \tag{38}$$

When the theoretical prediction of mass transfer coefficient is performed in bubble columns and airlift reactors with non-Newtonian fluids, the approach of the Ostwald-de Waele model is usually adopted (Kawase et al., 1987; Kawase and Hashiguchi, 1996; Tobajas et al., 1999). For Newtonian media ($n=1$; $k=\mu$; $\mu_c=\mu$ and $\alpha_r=0$), both Eqs. (37) and (38) are reduced to:

$$k_L = \frac{2}{\sqrt{\pi}} \cdot \sqrt{D_L}\left(\frac{\varepsilon \cdot \rho}{\mu}\right)^{\frac{1}{4}} \tag{39}$$

Garcia-Ochoa and Gomez (2005) have made the sensitivity analysis and the comparison between the values from the above equations and those given by available empirical k_L correlations, concluding that a good agreement is reached in general.

Kawase et al. (1992a) have applied Higbie's model, considering that the exposure time at a free surface of a fluid element in turbulent flows can be replaced for the sub-layer development time. They obtain the following equation for estimation of mass transfer coefficient:

$$k_L = \frac{4}{\sqrt{\pi}} \cdot 2^{\frac{1}{n}} \cdot \left(\frac{1}{T^+}\right)\sqrt{D_L}\left(\frac{\varepsilon \cdot \rho}{K}\right)^{\frac{1}{2\cdot(1+n)}} \tag{40}$$

5.2. Prediction of specific interfacial area

The interfacial area can be calculated from the values of the average bubble size, d_b, and the gas hold-up, ϕ, assuming spherical bubbles, by the following equation (Fukuma et al., 1987; Kawase et al., 1987; Wilkinson et al., 1994; Tobajas et al., 1999):

$$a = \frac{6\phi}{d_b} \tag{41}$$

The interfacial area can be increased by creating smaller bubbles or increasing the number of bubbles. For a given volume of gas, a greater interfacial area, a, is provided if the gas is dispersed into many small bubbles rather than a few large ones.

The specific interfacial area, a, is a strong function of the geometrical design and of the hydrodynamics into the bioreactor. Bioreactor design affects gas dispersion, hold up and the residence time of the bubbles. The properties of the medium also significantly affect the bubble sizes and coalescence and therefore the interfacial area.

The presence of solutes in the liquid phase, as is well known, can affect the mass transfer by changing the liquid phase physicochemical properties, disturbing the bubble coalescing behavior and the bubble size. In coalescent fluids (water or viscous liquids) the collisions among the bubbles lead to the formation of large bubbles which reduce the specific interfacial area. With an increase of viscosity, only the turbulent eddies with sufficiently high energy can penetrate through the boundary layer and the resistance to the mass transfer increases.

5.3. Specific interfacial area in stirred tank bioreactors

The stirrer speed and the mixing intensity play a major role in the breaking up of bubbles. As indicated before, the mechanical design of the bioreactor affects the gas dispersion, the hold-up and the residence time of the bubbles. Baffles are used to create turbulence and shear, which break up the bubbles. Although specific interfacial area values have been obtained by both physical and chemical methods, the accuracy of the measurement is generally very poor

(Kawase and Moo-Young, 1990). In the literature, several equations for the determination of the specific interfacial area in stirred tank reactors can be found (Joshi et al., 1982; Barigou and Greaves, 1996), although their application is very limited.

Gas hold-up, ϕ, can be estimated by the equation derived by Kudrewizki (1982) using the isotropic turbulence theory, as follows:

$$\frac{\phi}{1-\phi} = 0.5 \cdot \frac{V_s^{2/3}}{(gl)^{1/3}} \cdot \left(\frac{\rho_L}{\rho_L - \rho_G}\right) \tag{42}$$

In this equation, l is the Kolmogoroff length scale and, assuming that the size of the bubbles formed in the turbulent regime is affected by the stirrer speed, the following equation for l has been proposed (Kudrewizki and Rabe, 1986):

$$l = 2 \cdot \left(\frac{\sigma}{\xi \rho_L}\right)^{3/5} \cdot \left(\frac{L^{2/5}}{w^{6/5}}\right) \cdot \left(\frac{\rho_L}{\rho_G}\right)^{0.1} \tag{43}$$

where the coefficient of resistance, ξ, has a constant value of 0.4 for a wide range of Reynolds number values: $1 \cdot 10^3 \leq Re \leq 2 \cdot 10^5$.

Taking into account that the velocity on the blade is given by $w = \pi \cdot T \cdot N$, and for standard configurations: $L = \frac{1}{6} \cdot h$, the following equation can be derived:

$$\frac{\phi}{1-\phi} = 0.819 \cdot \frac{V_s^{2/3} N^{2/5} T^{4/15}}{g^{1/3}} \left(\frac{\rho_L}{\sigma}\right)^{1/5} \cdot \left(\frac{\rho_L}{\rho_L - \rho_G}\right) \cdot \left(\frac{\rho_L}{\rho_G}\right)^{-1/15} \tag{44}$$

When the liquid phase is viscous, the above equation needs to be modified to take into account the viscous forces neglected in the previous analysis (Bhavaraju et al., 1978; Kawase and Hashiguchi, 1996); the following equation can then be used:

$$\frac{\phi_v}{1-\phi_v} = \frac{\phi}{1-\phi} \cdot \left(\frac{\mu_L}{\mu_G}\right)^{-1/4} \tag{45}$$

In isotropic turbulent flow, the fluctuating velocity, u, is dependent on the length scale of the turbulent eddy at equilibrium, l, and on the rate of dissipation of energy per mass unit, ε, according to the following equation:

$$u = (\varepsilon \cdot l)^{1/3} \tag{46}$$

The dynamic pressure force can be expressed in terms of the fluctuating velocity, u, and assuming l to be of the same order of magnitude as the bubble diameter, d_b, and the following equation is obtained:

$$\tau \cong \rho_L \cdot u^2 \cong \rho_L \cdot \left[\left(\frac{P}{V}\right) \cdot \frac{d_b}{\rho_L}\right]^{2/3} \tag{47}$$

On the other hand, the equilibrium bubble diameter can be obtained by balance between the dynamic pressure force exerted on the bubble by the turbulent liquid flow, producing the bubble break-up, and the resistance forces (surface tension force and the resistance of the liquid phase to deformation, although the latter is usually small). The ratio between surface tension and turbulent fluctuation forces is the *Weber* dimensionless number, *We*, which can be assumed to have a constant value, according to:

$$We = \tau \cdot d_b / \sigma \tag{48}$$

Combining Eqs. (47) and (48), the following equation is derived:

$$d_b \propto \frac{\sigma^{3/5}}{\left(\frac{P}{V}\right)^{2/5} \cdot \rho_L^{1/5}} \tag{49}$$

In the literature many equations have been proposed for different systems using this relationship (Calderbank, 1958; Parthasarathy et al., 1991). Also, Bhavaraju et al. (1978) have found that bubble break-up depends on viscosity and liquid phase turbulence and have proposed the following equation for average bubble size:

$$d_b = 0.7 \cdot \frac{\sigma^{0.6}}{\left(\frac{P}{V}\right)^{0.4} \cdot \rho_L^{0.2}} \cdot \left(\frac{\mu_L}{\mu_G}\right)^{0.1} \tag{50}$$

where μ_G is the gas viscosity and μ_L represents the viscosity for pure Newtonian fluids.

5.4. Specific interfacial area in bubble columns and airlift bioreactors

The average bubble size in a bubble column has also been found to be affected by gas velocity, liquid properties, gas distribution, operating pressure and column diameter. Many literature correlations have been proposed to predict the hold-up (Hughmark, 1967; Kawase et al., 1992a) and size of bubbles (Calderbank, 1958; Calderbank, 1959). Kawase and Moo-Young (1990) and Kantarci et al. (2005) have reviewed these fluid-dynamic parameters of bubbles columns used for bioprocesses. Recently, Nedeltchev et al. (2007) have developed an empirical equation for estimation of a based on the geometrical characteristics (bubble length and height) of oblate ellipsoidal bubble formed in bubble columns with homogeneous regime under high pressure.

The gas hold-up is necessarily related to the superficial gas velocity and the mean bubble rise velocity, according to:

$$\phi = \frac{V_s}{U_S} \tag{51}$$

In airlift contactors the expression relating the gas hold-up in the riser to the liquid velocities and gas slip velocity can be written as (Garcia-Calvo and Leton, 1991):

$$\phi = \frac{V_s}{U_s + 1/2 V_{LC} + \bar{V}_{LR}} \tag{52}$$

where V_S is the superficial gas velocity, U_s is the terminal rise velocity of the bubble, V_{LC} is the average velocity in the core region and V_{LR} is the average linear velocity.

On the above equation, V_{LC} is calculated taking into account several assumptions, such as a parabolic profile for liquid velocity, the complete gas disengagement in the down-comer and hence, gas is not present in that reactor section (Garcia-Calvo and Leton, 1991).

The equilibrium bubble size under turbulence conditions can be calculated by Eq. (50) or be estimated from empirical equations. The most frequently used is that proposed by Calderbank (1958, 1959) for coalescent systems:

$$d_b = 4.15 \cdot \frac{\sigma^{0.6}}{\left(\frac{P}{V}\right)^{0.4} \cdot \rho_L^{0.2}} \cdot \phi^{0.5} + 9 \cdot 10^{-4} \tag{53}$$

and for non-coalescent fluids:

$$d_b = 1.93 \cdot \frac{\sigma^{0.6}}{\left(\frac{P}{V}\right)^{0.4} \cdot \rho_L^{0.2}} \tag{54}$$

For air water systems, the equilibrium bubble diameter, d_b, is usually assumed to be equal to 6 mm, and the gas the terminal rise velocity of bubble, U_s, to be equal to 0.25 $m \cdot s^{-1}$; both values are widely accepted in the literature (Tobajas et al., 1999).

5.5. Power input requirements

Power consumption is a significant part of the operating cost for large-scale systems. On the other hand, in order to determine k_L by Eqs. (37)–(39), the local energy dissipation rate, ε, near the interface needs to be estimated. It is assumed that energy at the gas–liquid

interface is consumed in the contact between liquid elements and gas bubbles. The power requirement for non-gassed Newtonian fluids is characterized by a dimensionless power number, *Np*, which is the ratio of the external force to the inertial force exerted by the fluid. It has been shown by dimensional analysis that the power delivered to an incompressible fluid by a rotating impeller in stirred tanks is proportional to the agitation rate raised to the third power and the impeller diameter raised to the fifth power (Rushton et al., 1950). Therefore, the average energy dissipation rate per mass unit in stirred tanks can be calculated as:

$$\varepsilon \approx \varepsilon_{ave} = \frac{P_0}{\rho\pi/4T^2H} = \frac{N_P N^3 T^5}{V} \tag{55}$$

There are many nonlinear correlations of N_P as function of Reynolds number and other dimensionless groups for different geometries of unaerated vessels (Masiuk et al., 1992; Netusil and Rieger, 1993). In laminar flow regime, the value of P_0, is inversely proportional to the Reynolds number value. In the turbulent regime ($Re > 10^4$), P_0 can be evaluated easily from experimental power curves, taking into account that the power number, N_P, can be considered constant, although its value depends on the stirrer type and geometry.

In gassed (aerated) systems, the presence of gas has an effect on power consumption. The sparged gas bubbles reduce density and therefore decrease power consumption. Thus, the power consumption in the case of aerated systems, *P*, is always lower than that consumed in an un-aerated system, P_o. Michel and Miller (1962) showed that for Newtonian fluids a good estimate of *P* can be obtained using the following relationship:

$$P = \alpha \cdot \left(\frac{P_0^2 \cdot N \cdot T^3}{Q^{0.56}}\right)^{\beta} \tag{56}$$

where the constants α and β depend on the stirrer type and on the configuration of the system agitation. Abrardi et al. (1988) have used this equation to describe experimental data in a wide range of operational conditions, obtaining values for α and β of 0.783 and 0.459 respectively, for a simple impeller Rushton turbine; while for dual impeller system the values are 1.224 and 0.432, respectively.

In order to use Eqs. (37)–(39) for estimation of k_L in bubble columns and airlifts, the power input from sparging air through a bioreactor must be obtained. In these systems, gas sparging must supply all the energy for the required bulk mixing and mass transfer. From the macroscopic energy balance on the gas phase at steady-state, the power consumption per liquid volume can be evaluated from:

$$\Delta\left(\frac{1}{2}\cdot U^2\right) + \Delta E_p + \int_{p_1}^{p_2}\frac{dp}{\rho_G} + \overline{W} + \overline{E_v} = 0 \tag{57}$$

where *U* represents the gas velocity; ΔE_P is the change of potential energy per mass unit; E_v means the frictional losses of energy per mass unit; and *W* is the work produced by the gas flow.

In the case of bubble column bioreactors, if the kinetic energy of the gas leaving the column and the frictional losses are assumed to be negligible, the following equation for pneumatic power input (Blanch and Clark, 1996; Sanchez et al., 2000) is obtained:

$$\frac{P}{V} = V_s \cdot \rho \cdot g \tag{58}$$

In airlift reactors the pneumatic power input can be obtained by following expression (Chisti and Moo-Young, 1998; Znad et al., 2004):

$$\frac{P}{V} = V_s \cdot \rho \cdot g \cdot \left(\frac{A_R}{A_R + A_D}\right) \tag{59}$$

where *P* is the power input due to the aeration; *V* is the culture volume; *g* is the gravitational acceleration; V_S is the superficial gas velocity based on the entire cross-sectional area of the reactor tube; and A_D and A_R down-comer and riser areas.

Garcia-Calvo (1989, 1992) has proposed a fluid-dynamic model for two-phase systems that predicts the energy dissipation at the gas–liquid interface, S, by using the following expression:

$$S = \phi \cdot V_s \cdot \rho \cdot g \cdot H \tag{60}$$

It is assumed that the energy dissipated at the gas–liquid interface is consumed in the contact between eddies and the gas bubble:

$$\varepsilon = \frac{S}{\rho \cdot H} = \phi \cdot V_s \cdot g \tag{61}$$

Thus, the volumetric mass transfer coefficient in bioreactors can be correlated and predicted taking into account the above equations for energy dissipated (Eqs. (55) to (61) and equations for mass transfer coefficient, k_L, (Eqs. (37)–(39)) and specific interfacial area, *a* (Eq. (41)).

5.6. Comrison between experimental and predicted k_La values

Frequently, broths are simulated with solutions of different substances with similar rheological properties using identical operational conditions and vessel geometrical parameters. Many fermentation media containing polymeric substances (such as polysaccharides) show non-Newtonian flow behavior. Most works on the subject have studied the effect of pseudo-plasticity on volumetric mass transfer coefficient in simulated culture broths (Perez and Sandall, 1974; Yagi and Yoshida, 1975; Nishikawa et al., 1981; Garcia-Ochoa and Gomez, 1998, 2001).

By combination of the equations for mass transfer coefficient, k_L, (Eqs. (37)–(39)) and specific interfacial area, *a*, (Eq. (41)) from gas hold-up,ϕ, (Eq. (45)) and average bubble size, d_b, (Eq. (50)) it is possible to predict the influence of operational conditions, properties of liquid and geometrical parameters of the vessels on the volumetric mass transfer coefficient, k_La. The capability of prediction of those equations has been checked making a comparison of k_La experimental values and some data obtained from correlations published for stirred tank reactors of different geometries, for Newtonian and non-Newtonian fluids (Yagi and Yoshida, 1975; Van't Riet, 1979; Chandrasekharan and Calderbank, 1981; Linek et al., 1991; Pedersen et al., 1994; Vasconcelos et al., 2000; Garcia-Ochoa and Gomez, 2001). As an example, in Fig. 8, k_La values predicted for Newtonian fluids for sparged stirred tank reactors for 50 L of volume are shown as a function of the power input per volume unit. In Fig. 9, the model predictions of k_La values for non-Newtonian systems are shown as a

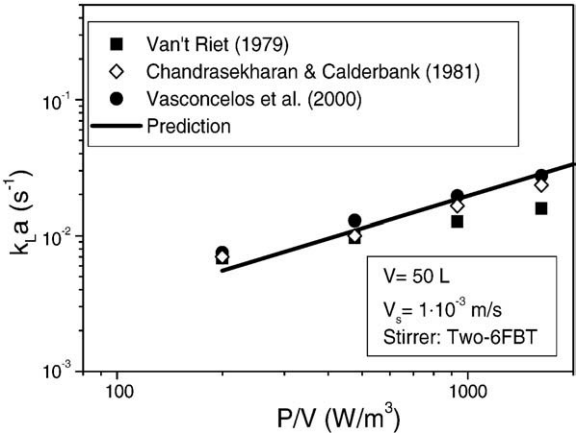

Fig. 8. Experimental data and model prediction of volumetric mass transfer coefficient values as a function of power input per unit volume for Newtonian liquids.

function of superficial gas velocity, V_S. Both figures include the results obtained by different authors for water and viscous liquids (xanthan gum solutions and sodium poly-acrylate). As can be observed, the k_La experimental values are in good agreement with those obtained using the proposed model.

Fig. 10 shows a comparison between some available data of k_La in stirred tank reactors and the values calculated by the proposed model over a wide range of vessel diameters (from $1.2\cdot10^{-2}$ to 1.5 m), for different stirrer types, for both Newtonian and non-Newtonian liquids (Van't Riet, 1979; Chandrasekharan and Calderbank, 1981; Nishikawa et al., 1981; Linek et al., 1991; Pedersen et al., 1994; Vasconcelos et al., 2000; Garcia-Ochoa and Gomez, 2001). As can be seen the differences between experimental and predicted values are lower than 15% in most cases.

On the other hand, Garcia-Calvo et al. (1999) have used a simple model to simulate the fluid-dynamic and mass transfer in a three-phase airlift reactor. The fluid-dynamic model is based on an energy balance which takes into account the energy dissipated at the interfaces. The mass transfer model is based on a previous two-phase fluid-dynamic model (Garcia-Calvo, 1992), the Higbie's penetration theory and the Kolmogorof's theory of isotropic turbulence.

Shimizu et al. (2000, 2001) have developed a phenomenological model for bubble break-up and coalescence in bubble column and airlift reactors. In order to describe bubble movements in a bubble column, a compartment concept is combined with the population balance model for bubble break-up and coalescence. The bubble column is assumed to consist on a series of discrete compartments in which bubble break-up and coalescence occur and bubbles move from compartment to compartment with different velocities. The volumetric mass transfer coefficient, k_La, was evaluated using the relationship for the specific surface area, a, related to gas hold-up and Higbie's penetration theory for k_L. The values given by the proposed model were in good agreement with the experimental data given in the paper and also with some available data in the literature. According to these authors, for the general applicability of this model in airlift bioreactors, data on gas hold-ups and volumetric mass transfer coefficients in larger external-loop reactors, including commercial-scale reactors, are highly desirable. Tobajas et al. (1999) have used a simple model to simulate the fluid-dynamic and mass transfer in a three-phase airlift reactor. The mass transfer model is based on a fluid-dynamic model which takes into account the energy dissipated at the phase interfaces (Garcia-Calvo, 1989, 1992; Garcia-Calvo and Leton, 1991; Garcia-Calvo et al., 1999), the Higbie's penetration theory and Kolmogoroff's theory of isotropic turbulence. Experimental data of gas hold-up, liquid velocity and volumetric mass transfer coefficient were simulated with satisfactory accuracy.

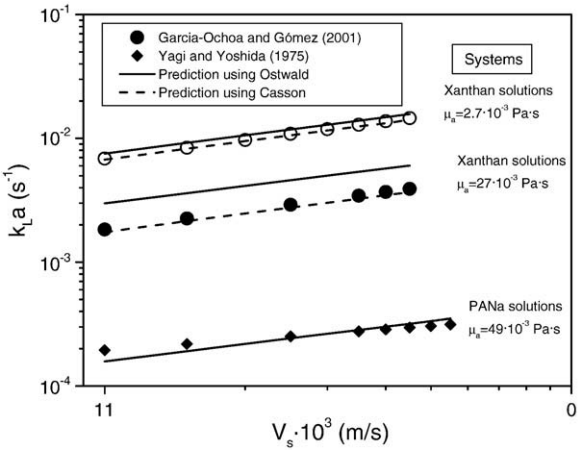

Fig. 9. Experimental data and model prediction of volumetric mass transfer coefficient values as a function of superficial gas velocity for different non-Newtonian systems.

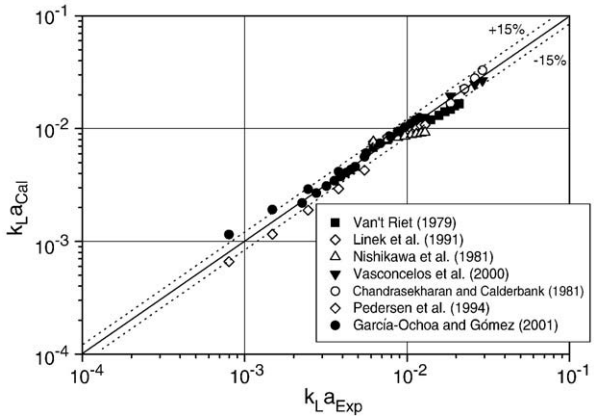

Fig. 10. Comparison between k_La values predicted by the proposed model and experimental data given in the literature (adapted from Garcia-Ochoa and Gomez, 2004).

6. Influence of oxygen consumption on k_La values

The study of oxygen transfer characteristic in fermentation broths has usually been separated into the parameters related to transport (studying the volumetric mass transfer coefficient, k_La, mainly) and the oxygen consumption by microorganism (determining OUR). However, correct prediction of OTR in a bioprocess must be made taking into account the relationship between both of them.

Vashitz et al. (1989) have reported that the oxygen transfer coefficient increases with the oxygen uptake rate of the microorganism in *X. campestris* cultures; Calik et al. (1997) have described the oxygen transfer effects on growth of *Pseudomonas dacunhae* for L-alanine production; and Calik et al. (2004, 2006) describes the oxygen transfer effects on benzaldehyde lyase production by *Escherichia coli*; all of them have found an enhancement on oxygen transfer rate due to the oxygen consumed by the microorganism. Djelal et al. (2006) have found that k_La values determined by the classical dynamic methods in sterile culture medium and after inoculation of culture, were of the same order of magnitude; however, the values were higher in presence of biomass ($0.0026\ s^{-1}$) compared to sterile medium ($0.0018\ s^{-1}$), since oxygen transfer was improved by its consumption by cells.

The variation of the specific gas absorption rate, per driving force and interfacial area units, due to the presence of the dispersed phase, in this case the microorganism, has been characterized by a biological enhancement factor, E. The following section is devoted to this factor.

7. Biological enhancement factor estimation

Taking into account the possible mass transfer enhancement over physical absorption in a biological system (due to the oxygen consumption by the microorganism), a biological enhancement factor, E, is defined as the ratio of the absorption flux of oxygen in the presence of a third dispersed phase (in this case the microorganism) to the absorption flux without it under the same hydrodynamic conditions and driving force for mass transfer, according to:

$$E = \frac{J}{J^0} = \frac{K_La}{k_La} \tag{62}$$

The extent of this enhancement can be derived for different theories for mass transfer; a simple model is the one corresponding to the film model. Some works in the literature have discussed the biological enhancement factor for oxygen absorption into fermentation broth, and

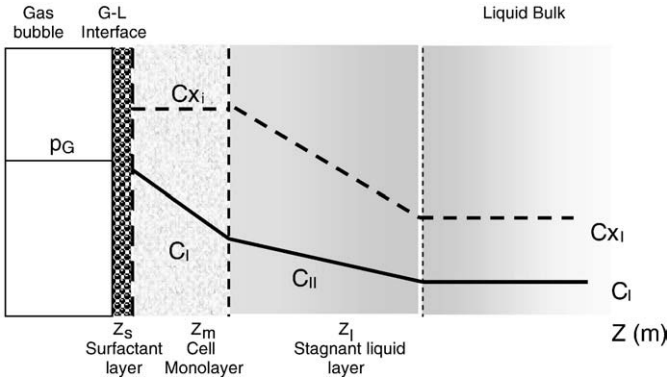

Fig. 11. Schematic representation of the steady-state profile of oxygen and biomass concentrations in a bioprocess (adapted from Garcia-Ochoa and Gomez, 2005).

several models with different cell concentration distribution have been used (Tsao, 1969; Merchuk, 1977; Ju and Sundararajan, 1992). Recently, Garcia-Ochoa and Gomez (2005) have proposed a model for the estimation of the biological enhancement factor in bioreactors. This model considers three layers in series; therefore, to describe the oxygen mass transport three mass transfer resistances are considered for the biological system (see Fig. 11): (i) the interfacial surfactant film resistance, (ii) the mono-layers of adsorbed microorganisms resistance, and (iii) the liquid film resistance. The different layer resistances are taken into account by the diffusion coefficient (D_i) by the inside of the layer and by layer thickness (z_i). According to this model, the biological enhancement factor, E, can be expressed as:

$$E = \left[1 + \frac{q_{O_2} Cx_m z_m^2}{2D_m(C^* - C_L)} \cdot \left(1 + 2 \cdot \frac{z_l D_m}{z_m D_L} + \frac{2z_L^2}{3z_m^2}\right) + \frac{1}{3} \cdot \frac{q_{O_2} C_{X_L} z_L^2}{2D_l(C^* - C_L)}\right] \cdot \left[\frac{z_L/D_L}{\sum_i z_i/D_i}\right] \quad (63)$$

where $C_{X,i}$ represents the cell concentration in the cell mono-layer or in the continuous phase in liquid film; D_i is the molecular diffusion coefficient within a film of thickness z_i; q_{O2} represents the specific oxygen uptake rate of microorganism; C_L and C^* are the oxygen concentration in the liquid and in equilibrium with the air stream, respectively.

The first bracket in Eq. (63) is always ≥1 and is a function of the *Hatta* number, taking into account the transport enhancement due to the oxygen uptake by the microorganisms. The *Hatta* dimensionless number is given by (Merchuk, 1977; Garcia-Ochoa and Gomez, 2005):

$$Ha_i = \frac{q_{O_2} C_{X,i} z_i^2}{2D_i \cdot (C^* - C_L)} \quad (i = L, m) \quad (64)$$

The second bracket of Eq. (63) is ≤1, representing the physical blocking effect due to the absorbed surfactant film, the cell adsorption to the bubbles surface, considering those as semi-permeable solid particles hindering the movement of diffusing oxygen molecules, and the liquid film. Depending on the relative values of both terms, the enhancement factor, E, can take values smaller than, equal to or bigger than 1.

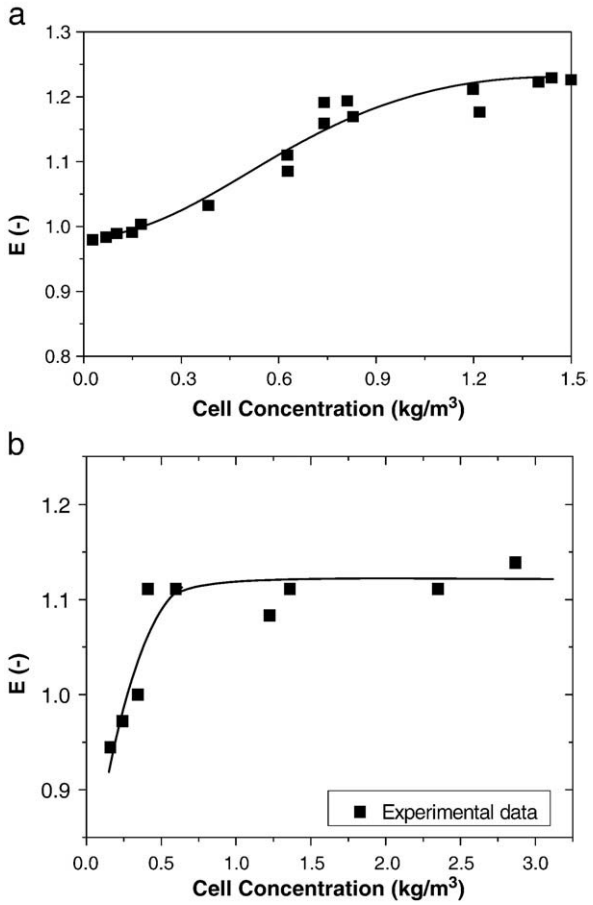

Fig. 12. Biological enhancement factor: experimental and estimated values from Eq. (63) in cultures of: a) *Xantomonas campestris* b) *Rhodoccocus erythropolis* (adapted from Garcia-Ochoa and Gomez, 2005).

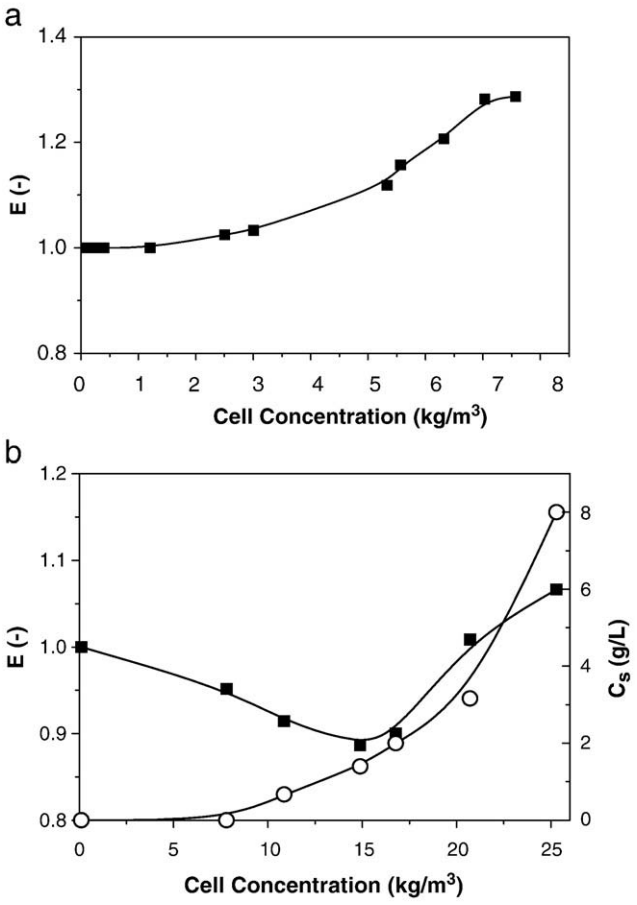

Fig. 13. Biological enhancement factor: experimental and estimated values from Eq. (63) in culture of *Candida bombicola*: a) growth medium, b) production medium (adapted from Garcia-Ochoa and Gomez, 2005).

Figs. 12 and 13 show some experimental values of E (calculated by the ratio of the experimental oxygen mass transfer coefficient in the presence of microorganism, K_La, and that measured into the same medium in the absence of biomass at different conditions of oxygen transfer, k_La). As can be observed, the E values obtained in the presence of biomass can be higher than 1. The values $E<1$ indicate that mass transfer is accompanied by a slow uptake rate and a greatest resistance to transport by the serial resistances above commented. Also, biological enhancement factor values have been estimated from Eq. (63) and represented in the same Figs. 12 and 13 as lines; as can be seen the agreement between experimental and predicted values is good.

8. Scale-up and oxygen transfer rate in aerobic bioprocesses

As already indicated, the oxygen transfer rate can control the overall rate of the bioprocess, and as a consequence, it can determine the capacity of a bioreactor. For this reason the oxygen transfer rate condition has been often chosen as the main criterion for scaling-up. The prediction of the results to be obtained in an industrial scale, from the data collected in laboratory or pilot plant scales, requires a careful analysis of the influence of the operational conditions on the biological behavior of the system.

Key to scale-up using constant oxygen transfer rate (OTR) is the ability to measure or estimate the volumetric mass transfer coefficient, k_La. A high number of correlations are available for the volumetric mass transfer coefficient, but often the results from different equations are not in agreement with others (Garcia-Ochoa and Gomez, 1998; Gogate et al., 2000; Sanchez et al., 2000). Therefore they are being displaced by theoretical or predictive models, based on more fundamental principles.

In a bioprocess, according Eqs. (1) and (62), the oxygen mass transfer rate, N_{O2}, can be rewritten as:

$$N_{O_2} = a \cdot J = a \cdot E \cdot J^0 = k_G a \cdot (p_G - p_i) = E \cdot k_L a (C_i - C_L) \tag{65}$$

where J is the absorption flux of oxygen in presence of microorganism, a is the interfacial area, k_G and k_L are mass transfer coefficient and E is the biological enhancement factor.

Considering the overall volumetric mass transfer coefficients, it can be written:

$$N_{O_2} = K_G a \cdot \left(p_G - p^*\right) = K_L a \cdot \left(C^* - C_L\right) \tag{66}$$

being:

$$\frac{1}{K_L a} = \frac{1}{H \cdot k_G a} + \frac{1}{E \cdot k_L a} \tag{67}$$

It can be observed that the overall volumetric mass transfer coefficient in the presence of a biochemical reaction, K_La, is a lumped parameter comprising the resistance to mass transport of oxygen due to gas and liquid phase resistances, and also due to the oxygen consumption, which can be taken into account by a biological enhancement factor, E. Assuming that the gas phase resistance can usually be neglected, the overall resistance to transport can be written as:

$$K_L a = E \cdot k_L a \tag{68}$$

When biochemical reaction does not take place or when its rate is not much greater than the mass transfer rate, $E=1$ and the overall mass transfer coefficient will be denoted by k_La and the flux by J^o.

Thus, volumetric mass transfer coefficient in bioreactors can be predicted considering theoretical equations for k_L (Eqs. (37)–(39)) and a (Eq. (41)) coupled to the equation for the estimation of the biological enhancement factor, E (Eq. (63)). The input parameters necessary can be categorized into four groups:

i. the system physical properties (μ_L, σ, ρ_L, D_L, C^*);
ii. the biochemical properties (Cx_m, z_m, q_{o2});
iii. the operational conditions (V_S, N, P/V),
iv. and the geometrical parameters of bioreactor (kind and size of bioreactor, design and number of stirrers, etc.).

The parameters in the first two groups are determined by the nature of the system and can not be altered freely; the last two groups depend on the process parameters and on the device used.

There are five different items needed for the design of bioreactors (Kawase and Moo-Young, 1990): Stoichiometry, thermodynamics, microbial kinetics, transport phenomena (heat and mass transfer) and economics. Stoichiometry, thermodynamics and kinetics are scale-independent phenomena. Transport phenomena and economics are highly dependent on scale. Moreover, usually mass transport rates govern the aerobic bioprocess overall rate.

Scale-up is a procedure for the design and construction of a large scale system (where the scale is typically from 30 to1000 m^3) on the basis of the results of experiments with small-scale equipment (where the scale is typically from 1 to 25 L). The scale-up of a bioprocess can be classified into three main scales (Ju and Chase, 1992, Junker, 2004): i) *laboratory*, where elementary studies are carried out; ii) *pilot plant*, where the bioprocess optimizations are determined; and iii) *production scale*, where the bioprocess is brought to economic realization. Recently, the *shake-flask* and *micro scales* can be added to the list (Micheletti et al., 2006), some characteristics of mass transfer in miniature bioreactors are commented in the following sub-section.

8.1. OTR in miniature bioreactors. Scale-up and scale-down

Bioprocess development (strain selection, strain enhancement, process optimisation) has traditionally required the screening of large numbers of cell lines in shake flask cultures. Afterwards, further testing of successful candidates in *laboratory scale* bioreactors prior to *pilot plant* studies is usually performed. The need for carrying out a vast number of cultures has resulted in the increasingly widespread development of *shake-flask* and *micro scale* bioreactor systems. These systems offer a miniaturised, high-throughput solution to bioprocess development.

Miniature bioreactors (MBRs) can reduce the labour intensity and material costs of the vast number of fermentative experiments necessary in bioprocess development, increasing the level of parallelism and throughput achievement, both highly interesting areas (Lamping et al., 2003; Doig et al., 2005; Betts and Baganz, 2006; Zhang et al., 2007; Gill et al., 2008; Li et al., 2008). It is important that such devices be very reliable to accurately mimic laboratory and *pilot scale* bioreactors when used for bioprocess development. Therefore, growth kinetics and product formation – optimised at *micro scale* – can be expected to be scaled-up quantitatively. Work by Micheletti et al. (2006) shows that scale translation from shaken to stirred systems is feasible if scale-up criteria are carefully chosen. These results provide initial data on satisfactory scale up of a mammalian cell culture process, using a constant mean energy dissipation rate. Moreover, the *micro scale* device reported by Lamping et al. (2003) was a scaled-down version of conventional stirred tank bioreactors machined from Plexiglas and equipped with four baffles, stirrer and sparger.

Betts and Baganz (2006) have compared different reported MBRs illustrating performance specifications and its description based on their agitation system, considering the type of conventional bioreactors either imitated or derived from. According to these authors, MBRs can be classified in shaken (flask, microtiter and spin tubes), stirred, bubble column miniature bioreactors and other miniature devices.

Many techniques have been applied for determination of k_La in MBRs. In fact, the dynamic method of gassing-out is the most usual method. The values reported (up to 0.4 s^{-1}) depend on the miniature bioreactors used, and the efficiency of agitation and aeration systems.

Doig et al. (2005) estimated k_La by three methods (the dynamic gassing out method, by mass balance of the inlet and exit gasses, and by mass balance from the growth rate under oxygen limitation in *Bacillus subtilis* cultures) in a prototype miniature bubble column bioreactor. There are also specific methods available for determining k_La at *micro scale* devices which provide data that are directly comparable with values obtained under actual process conditions. Thus, Duetz et al. (2000) and Duetz and Witholt (2004) estimated OTR by mass balance under conditions of oxygen limitation from the linear growth of *Pseudomonas putida* and by enzymatic oxidation of glucose coupled to a secondary reaction in microtiter plates. Recently a novel method based on the bio-oxidation of catechol by the enzyme catechol-2,3-dioxygenase has been reported (Ortiz-Ochoa et al., 2005).

The most commonly used culture vessel in bioprocess development is the shaken flask: Erlenmeyer flasks (100–2000 ml) filled with low volumes of media (10–25%) are shaken to promote fluid mixing and gas–liquid mass transfer via surface aeration. Therefore, the major limitation of shake flasks is their dependence on surface aeration, leading to reduced oxygen transfer compared to that achieved in stirred tank bioreactors. Liu et al. (2006) have measured k_La values in the shake-flasks (using the sulphite method). They found that k_La decreases with the liquid volume in flask and increases with the shaker speed. In this study k_La was correlated to shaker speed and liquid volume by the following equation:

$$k_La = 0.141N^{0.88}\left(\frac{V_L}{V_o}\right)^{-0.80} \quad (69)$$

The small difference in absolute values of the indices on N and V_L implies that the two variables have a similar impact on the oxygen transfer rate.

Several changes to the conventional Erlenmeyer flask have been proposed in order to increase oxygen mass transfer. Kato and Tanaka (1998) incorporated gas-permeable membranes in the upper corners of their prototype flasks, which allowed a more effective gas flow into the vessel during shaking. This modification overcame the problem found in conventional shake flasks when the addition of more sterile air into the system is needed to avoid inhibition of microbial growth due to oxygen depletion. k_La values of 0.042 s^{-1} (600 mL, 200 rpm) to 0.077 s^{-1} (100 mL, 200 rpm) were recorded in a novel, box-shaped, shake flask system.

In bioprocesses carried out in stirred tank bioreactors when the oxygen uptake rate is high, the introduction of baffles can increase OTR due to increasing power input (Peter et al., 2006). However, hydrodynamic stress produced in both baffled and unbaffled shake flasks could slow down the growth rate (Garcia Camacho et al., 2007) or alter production rates, e.g. production of 6-pentyl-α-pyrone by *Trichoderma harzianum* (Galindo et al., 2004).

The use of shaken microtiter plates (microplates) is becoming a good alternative to the shaken flask. Limits to these new systems are the relatively low rates of oxygen transfer, complexities with instrumentation and scaling-up difficulties. Microtiter plates can either be rectangular or cylindrical, with square geometries improving mixing and oxygen transfer by mimicking the action of baffles. A major determinant of good oxygen transfer is the shaking amplitude and frequency, as well as the shape and size of the wells. The square shape in the horizontal plane results in a turbulent shaking pattern and, therefore, better mimics the situation in stirred tank bioreactors than round well microtiter plates do. Maximum OTR of about 16.4 mmol L^{-1} h^{-1} in round wells and 38 mmol L^{-1} h^{-1} in square deep-well microtiter plates (k_La between 0.028 and 0.052 s^{-1}) have been reported (Duetz et al., 2000; Duetz and Witholt, 2004).

Recently spin tubes have been developed and used as a *small scale* process development tool for cultivation of mammalian cells. The relatively large volume and low evaporation rate found in this device are adequate for dealing with slow-growing mammalian cells, where cultures can be many days in duration. The most critical parameters in these cultures are pH and dissolved oxygen concentration. Nevertheless, De Jesus et al. (2004) have found that the interval of change of oxygen concentration and pH during cultures in spin tubes are comparable to those observed in more sophisticated and bigger bioreactors.

Miniature stirred bioreactors (MSBRs) based on conventional stirrer tank reactors have been developed as an alternative to shaken MBR systems for early-stage process development and cell characterisation. By providing agitation and aeration of the vessel, mass transfer rates close to a conventional *laboratory scale*. Lamping et al. (2003) have predicted (modelling oxygen transfer from Higbie's model with the contact time obtained from the computational fluid dynamics) and they have measured (using the dynamic method) k_La in a prototype MSBR, obtaining values in the range 0.028 to 0.11 s^{-1}. Gill et al. (2008) have studied oxygen mass transfer characteristics as a function of stirrer speed and aeration rates in a miniature bioreactor geometrically similar to conventional *laboratory scale* stirred bioreactors, with k_La values up to 0.11 s^{-1}. Results achieved could be comparable to those found in typical laboratory scale bioreactors.

As a novel alternative to shaken vessels at *small scale* and high throughput cell culture, a miniaturized bubble column reactor (MBCR) has been developed. This reactor is based on an MTP with porous membranes acting as the entire base to each individual well. The mechanical simplicity coupled with potentially high oxygen transfer rate and ease of sampling makes MBCRs suitable for parallel cell cultivation. Doig et al. (2005) have used a microplate bubble column bioreactor that is capable of supporting the aerobic growing of *Bacillus subtilis* in a working volume of 2 mL. k_La values were reported up to 0.061 s^{-1} using the dynamic gassing-out method at a superficial gas velocity of 0.02 m s^{-1}. Experimental data of k_La fitted to Eq. (32) found:

$$k_La = 0.65 \cdot V_S^{0.6} \quad (70)$$

As indicated above, it can observed (Table 5) that the effect of the superficial gas velocity on k_La is similar to that in bubble column bioreactors.

Thus, MBR technology promises to enable faster, less labour intensive bioprocess development, with a huge reduction in reactive amount needed and, thus, waste generation. However, there is no single MBR that satisfies all requirements equally, for OTR mainly. In fact, there is a need to differentiate *micro scale* systems and the advantages that each one confers depending on the application. Therefore, different systems for different stages of the development of a bioprocess can be used, taking into account its complexity and the nature of the cells, especially the requirements of dissolved oxygen for growing, monitoring, control, and sampling.

8.2. Bioreactor scale-up

Once a particular bioprocess is accomplished successfully in *laboratory scale* experiments, the values of the operating variables and the physical properties are known or can be measured. The bioprocess is then usually carried out in a number of bioreactors of increasing scale, the final process optimization being performed at pilot plant scale (50 to 300 L of volume) where the operational conditions and the hydrodynamic and mixing are very similar to those used in the production scale. The scale-up ratio is typically about 1:10 for bioprocesses, but lower ratios decrease the risk of unexpected performance on scale-up. It can be done according to four different approaches, as widely recognized: fundamental methods; semi-fundamental methods; dimensional analysis; and rules of thumb.

Fundamental methods are those based on the application of mathematical models for description of the influence of operational conditions and geometrical design of the bioreactor on the flow pattern in the bioreactor. Solution of the microscopic balances of

Table 9
Different criteria for bioreactor scale-up (adapted from Oldshue, 1966)

Variable	Value of volume at model system (2 L)	Value of volume at pilot scale (20 L)			
		Scale-up criteria			
		$P/V=C$	$\pi NT=C$	$Re=C$	$k_La=C$
T	1.0	2.14	2.14	2.14	2.14
P	1.0	10.0	4.80	0.50	13.8
P/V	1.0	1.0	0.48	0.05	1.38
N	1.0	0.60	0.47	0.22	0.67
$N{\cdot}T$	1.0	1.28	1.0	0.47	1.43
Re	1.0	2.75	2.15	1.0	3.07
k_La	1.0	0.77	0.55	0.19	1.0

momentum and mass transfer is required. In recent years, computational fluid dynamics has shown to be an effective tool to study the hydrodynamics of reactors and scale-up of bioprocesses (Dhanasekharan et al., 2005). These methods are very complicated, and frequently, many simplifications are required (Vasconcelos et al., 1998; Nedeltchev et al., 1999). Nevertheless, the development of fundamental models able to describe the key characteristics of the system is perhaps the most helpful tool for successful scale-up and for the determination of the optimal conditions at the production scale.

Semi-fundamental methods are those where simplified equations are applied to obtain a practical approximation to the bioprocess operation. The parameters obtained will be scale dependent, and thereby the influence of scale on the process can be examined by model simulations. However, despite the extensive simplification of the problem when moving from the fundamental to semi-fundamental models, the complexity of the method is still substantial.

Dimensional analysis is based on keeping the values of dimensionless groups of parameters constant during the scale-up. The dimensionless groups used are ratios of rates or time constants for the different mechanisms involved in bioprocess. Then, if all the dimensionless groups are kept constant, the relative importance of the mechanisms or phenomena involved in the process will not change during scale-up. It is often impossible to keep all the dimensionless groups constant during scale-up, hence one has to determine the most important groups and deemphasize the rest.

The rule of thumb method is the most common method. The scale-up criterion most used and percentage of each criteria used in the fermentation industry are: constant specific power input, P/V, (30% of use); constant volumetric mass transfer coefficient, K_La (30%); constant impeller tip speed of the agitator or shear (20%); and constant dissolved oxygen concentration, C_{O2}, (20%) (Margaritis and Zajic, 1978). The different scale-up criteria normally result in entirely different process conditions on a production scale. Usually, it is impossible to maintain all the parameters in the same ratio to one another. The consequences of such calculations, for two geometrically similar stirred tank reactors with the model system volume (V=2 L) and the production system volume, (V=20 L) with linear scale-up factor of 10 are shown in Table 9. Analysis of the obtained results shows that, for instance, scale-up based on constant P/V will increase the maximum shear rate by 28% (ND=1.28) and using a constant Re number value is not a good scale-up criterion, because a very low P/V value results (P/V=0.05), which can provoke a deficient mixing. Agitator tip speed like criteria has some advantages in the case of bioprocesses with sensible micro-organisms over shear stress produced by stirrer, because it determines the maximum shear stress in the tank, determining the possible cell damage, and also influences the stable size of flocks and gas bubbles. However, its use entails a reduction in the power input per unit volume and in the stirrer speed, which causes a remarkable reduction of the rate of oxygen transport. Therefore, it seems that the best criteria for scale up is to maintain the power input per unit volume or the volumetric mass transfer coefficient constant (Figueiredo and Calderbank, 1979; Shukla et al., 2001). Thus, application of the rule of thumb method is very simple, but it is also a very fragile method, because a complete change in the limiting regime can happen above a certain scale.

In practice, all four methods are used in combination with each other and sometimes the trial and error method must also be included. In general, it is impossible to scale up a bioprocess keeping all conditions in the optimal values and it is necessary to choose which variable is considered as the most important. Junker (2004) has evaluated the different scale-up methods and approaches that have been applied to *Escherichia coli* and yeast processes, finding that scale-up from the 30 L laboratory scale typically under-predicted parameters of industrial production and 280 L scale up parameters were most similar to the *production scale*.

For the scale-up of aerobic fermentation, the effect of gas liquid mass transport is the most significant factor. Therefore, scale-up in aerobic fermentation is often performed on the basis of keeping the volumetric mass transfer coefficient (k_La constant) or, if C_L is negligible compared with C^* in the culture broth, keeping OTR constant (Herbst et al., 1992; Garcia-Ochoa et al., 2000a; Shukla et al., 2001; Bandaiphet and Prasertsan, 2006; Liu et al., 2006b). The success of the scale-up processes are usually confirmed by experimental results which show that there is no difference between small and large scale fermentation carried out under the same oxygen transfer rate.

On the other hand, although the kinetic parameters of growth and oxygen consumption of microorganism must be scale independent, the growth rate in a bioreactor is scale dependent because of the scale dependency of oxygen transport rate. Another aspect making the situation more complex is that some operational conditions necessary for adequate mass transfer can produce negatives effects. The local environment of the cells in large industrial bioreactors varies over a higher range than in small laboratory bioreactors, because of the higher heterogeneity of the cultivation medium caused by the longer global mixing time, the turbulence intensity, and thus local shear

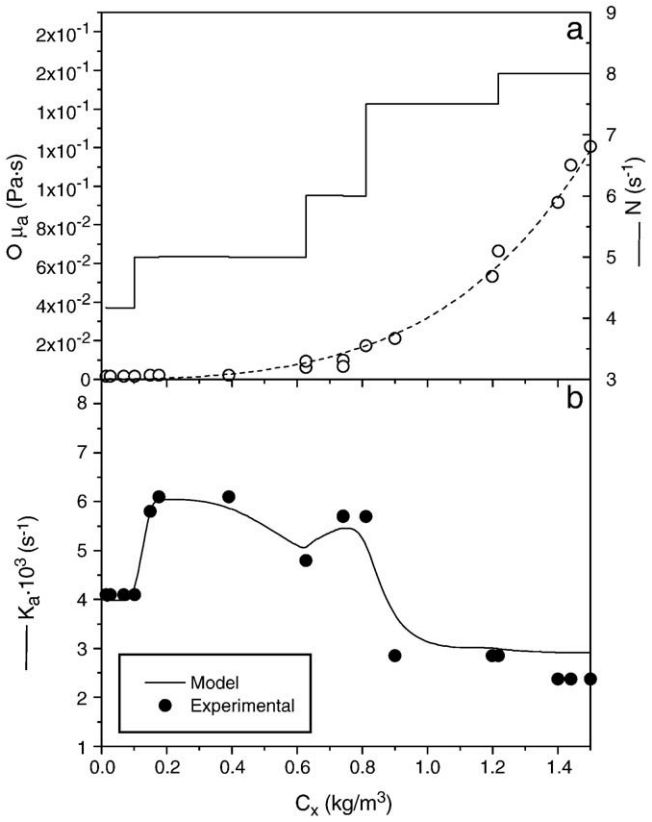

Fig. 14. Evolution of apparent viscosity and volumetric mass transfer coefficient on the course of fermentation of *Xanthomonas campestris* during xanthan gum production (using an increasing of stirrer speed) (adapted from Garcia-Ochoa and Gomez, 2005).

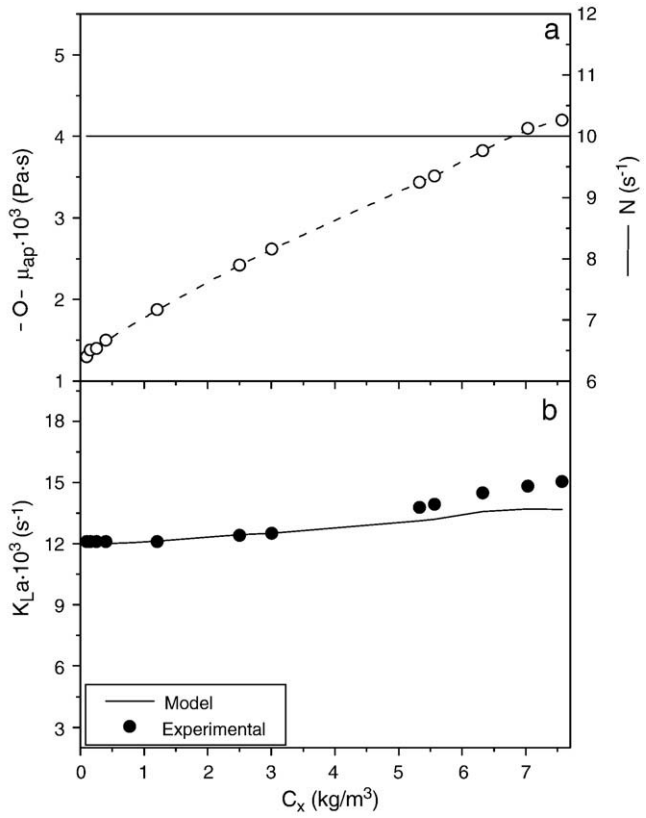

Fig. 15. Evolution of apparent viscosity and volumetric mass transfer coefficient on the course of fermentation in growth medium of *Candida bombicola* (using a constant stirrer speed of 10 s^{-1}) (adapted from Garcia-Ochoa and Gomez, 2005).

forces are exacerbated with the increasing scale of bioreactors; under these conditions, cellular stress can affect growth (Kieran et al., 2000). For the scale-up of toyocamycin production by a shear-sensitive mutant of *Streptomyces chrestomyceticus* the OTR constant method could be not used and thus scale-up was done at the lowest possible tip speed for the geometrically similar larger vessel (Flickinger et al., 1990).

The oxygen transfer rate into the microbial cell in aerobic bioprocesses strongly affects growth and product formation by influencing metabolic pathways and changing metabolic fluxes (Calik et al., 2004; Martin et al., 2005; Gomez et al., 2006); therefore, to fine-tune bioreactor performance in relation with the physiology of the microorganism and operational conditions for the extent of oxygen transfer, the requirement must be clarified.

When the mass transfer coefficient, k_La, is relatively high, no influence of the oxygen uptake by the microorganism can be detected because the enhancement is very small. However, the situation may change in the case of cultures with high oxygen uptake rate or with high viscous broth, where the decrease of k_L together with the activity of the microorganism enhances oxygen mass transfer, and k_La observed is increased significantly compared to physical absorption (inert conditions).

Xanthan production by *X. campestris* cultivation is an example of this kind of systems. Xanthan gum fermentation includes an important influence of viscosity broth on mass transfer rate during the production process (Garcia-Ochoa et al., 2000b). As an example, Fig. 14 shows a comparison between experimental and predicted K_La values, taking into account changes on operational conditions in time course of batch fermentation. Fig. 14a shows the dramatic increase of viscosity of the broth, which enlarges film resistance to transport, and produces the decreasing of oxygen mass transfer coefficient, k_L; in consequence, an increasing of stirrer speed is necessary to maintaining an adequate dissolved oxygen concentration. Fig. 14b shows a comparison between experimental and predicted values of K_La, taking into account all the effects above commented: change in viscosity broth (for xanthan production) and change in the stirrer speed, together with the evolution of other magnitudes (biomass concentration and OUR).

Using another example, in sophorolipids synthesis by yeast *Candida bombicola* (a biosurfactant, product non-associated to growth) the oxygen concentrations also have an important role. Fig. 15a shows the moderate variation of viscosity of the broth, caused by the increasing of biomass concentration, for a constant stirrer speed of 10 s^{-1}. In Fig. 15b the evolution of the volumetric oxygen mass transfer, K_La, with the biomass concentration during time course fermentation of yeast growth and the values predicted by the model are presented. When sophorolipids are produced and segregated into the medium, the surface tension decreases until the micelle critical concentration is reached. Under those conditions K_La also decreases reaching a value of $9.4 \cdot 10^{-3}$ s^{-1}. Then, for large cell concentrations, which mean that OUR increases, the volumetric mass transfer coefficient value also increases because the enhancement factor increases, assuming values higher than 1. Fig. 16 is an example of the evolution of different mass transport parameters during the production of sophorolipids by *C. bombicola*. Fig. 16a shows the variation of the sophorolipid concentration and the surface tension in time course of fermentation and in Fig. 16b the experimental and predicted K_La values are shown during the biosurfactant production.

In *Rhodococcus erythropolis* cultures, the growth of the bacteria is also strongly dependent on the availability of oxygen. The dissolved oxygen concentration is dependent on the oxygen transfer rate from the air bubbles to the liquid and on the oxygen uptake rate for growth,

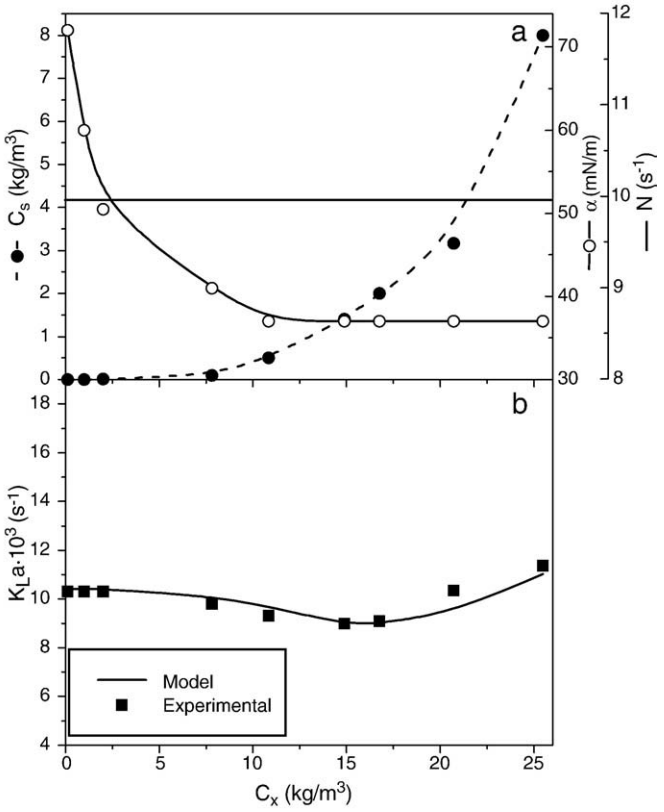

Fig. 16. Evolution of surfactant concentration, surface tension and volumetric mass transfer coefficient on the course of fermentation of *Candida bombicola* for sophorolipid production (using a constant stirrer speed of 10 s^{-1}) (adapted from Garcia-Ochoa and Gomez, 2005).

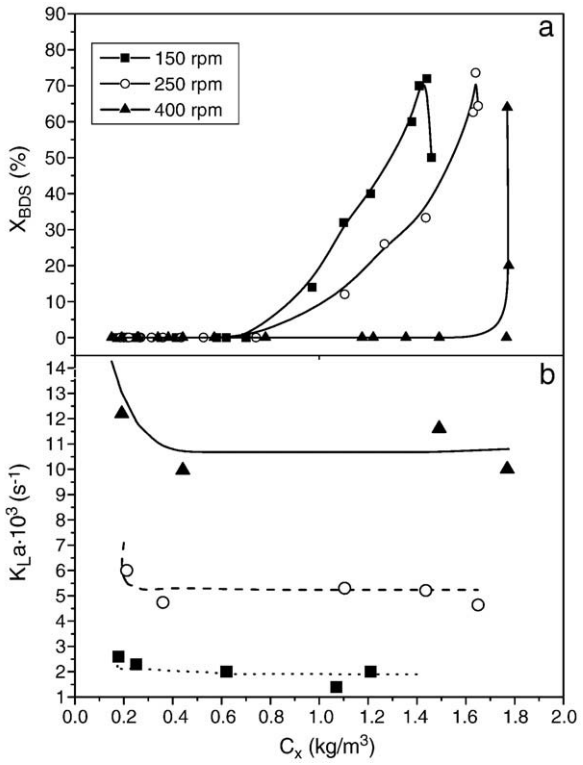

Fig. 17. Evolution of biodesulphurization capability and volumetric mass transfer coefficient on the course of fermentation of *Rhodococcus erythropolis* (for different stirrer speeds) (adapted from Gomez et al., 2006).

maintenance and biodesulphurization capability accumulation by the cells (Olmo et al., 2005; Gomez et al., 2006). In Fig. 17a experimental values of biodesulphurization capability of the cells under different mass transfer conditions (due to the change in stirrer speed) *versus* biomass concentration are represented; it can be seen that the maximum percentage of desulphurising capability is similar for stirrer speeds between 250 to 400 rpm (approximately of 80% for cells grown during 30 h). In the case of working at 150 rpm, this decrease is faster, surely as a consequence of the oxygen transport limitation during growth. Finally, experimental and predicted K_La values, under different operational conditions, are shown in Fig. 17b. Again, theoretical predicted model values for k_La and E yield satisfactory results when experimental and predicted values are compared.

A reasonable agreement is found between the experimental data and the values predicted by the theoretical model described, for sparged and stirred tank bioreactors, under a wide range of operational conditions, for different cultures of *X. campestris* (producing xanthan, a polysaccharide), *C. bombicola* (a yeast producing a sophorolipid or bio-surfactant) and *R. erythropolis* (bacteria with biodesulphurization capability).

OTR is the most important parameter implied on the design, operation and scale up of bioreactors. Aerobic bioprocesses involve transport and biochemical reactions of one or more species simultaneously. A proper mechanical design of the bioreactor is very important to provide a controlled system where a homogeneous oxygen concentration in the medium lets us achieve an optimal growth and/or a product formation. In this way, aeration and agitation are important variables in order to produce an effective oxygen transfer rate into the medium and oxygen uptake rate must be known in order to control the dissolved oxygen concentration. Thus, in order to have an adequate description of bioprocesses, the knowledge of the volumetric mass transfer coefficient value, as characteristic parameter of the OTR, is required, taking into account the different aspects considered in the present review.

Nomenclature

a	Specific interfacial area (m^{-1})
a, b, c, d, e	Exponents in Eqs. (31) to (33)
A_D	Down-comer cross-sectional area (m^2)
A_R	Riser cross-sectional area (m^2)
C	Concentration ($kg \cdot m^{-3}$); Constant of empirical Eqs. (31) to (33)
c	Constant defined in Eq. (28)
CMC	Carboxymethyl celulose
C_X	Biomass concentration ($kg \cdot m^{-3}$)
D	Diameter of bioreactor, vessel or column (m)
d_b	Bubble diameter (m)
D_i	Oxygen diffusion coefficient in layer i ($m^2 \cdot s^{-1}$)
E	Biological enhancement factor (–)
E_P	Potential energy per mass unit ($J \cdot kg^{-1}$)
E_v	means the frictional losses of energy per mass unit ($J \cdot kg^{-1}$)
F	Molar flow rate ($mol \cdot s^{-1}$)
g	Gravitational constant ($m \cdot s^{-2}$)
H	Henry constant ($mol \cdot m^{-3}$ atm^{-1}); Height (m)
h	Blade height of stirrer (m)
Ha	Hatta number (–)
J	Flux density molar ($mol\ O_2 \cdot m^{-2} \cdot s$)
k	Consistency index in a power-law model ($Pa.s^n$)
k_L	Mass transfer coefficient ($m \cdot s^{-1}$)
K_La	Volumetric oxygen mass transfer coefficient in presence bio-transformation (s^{-1})
k_La	Volumetric oxygen mass transfer coefficient (s^{-1})
l	Kolmogoroff length scale (m)
N	Stirrer speed (s^{-1})
n	Flow index in a power-law model (–)
N_l	Normal stress ($N \cdot m^{-2}$)
N_P	Power dimensionless number (–)
OUR	Oxygen uptake rate ($mol\ O_2 \cdot m^{-3} \cdot s^{-1}$)
P	Power input under gassed conditions (W)
PANa	Sodium poly-acrylate
P_o	Power input in un-aerated systems (W)
P	Pressure (Pa)
Q	Gas flow rate ($m^3 \cdot s^{-1}$)
Re	Reynolds number (–)
S	Energy dissipation at the gas–liquid interface ($W \cdot m^{-2}$)
T	Stirrer diameter (m).
t	Time (s)
t_e	Exposure time (s)
U	Gas velocity ($m \cdot s^{-1}$)
Us	Terminal rise velocity of bubble liquid circulation velocity ($m \cdot s^{-1}$)
u	Root mean square of fluctuation velocity ($m \cdot s^{-1}$)
V	Volume of the liquid in the vessel (m^3)
V_o	Volume of flask (m^{-3})
V_{LR}	Average liquid circulation velocity ($m \cdot s^{-1}$)
V_{LC}	Average velocity in the core region ($m \cdot s^{-1}$)
V_S	Superficial gas velocity ($m \cdot s^{-1}$)
W	Work produced by the gas flow ($J \cdot kg^{-1}$)
We	Weber dimensionless number (–)
w	Velocity of blade ($m \cdot s^{-1}$)
X_{BDS}	Percentage of biodesulphurizationz film thickness or distance from the gas–liquid interface (m)

Greek letters

α_r	Apparent yield stress to shear stress ratio in Eq. (38)
γ	Shear rate (s^{-1})
ε	Energy dissipation rate ($W \cdot kg^{-1}$)
η	Eddy length (m)
ϕ	Gas hold-up (–)
ϕ_v	Gas hold-up in viscous system (–)
λ	Characteristic material time (s)

μ	Viscosity (Pa·s)
μ_a	Apparent viscosity according to the Ostwald-de Waele model (Pa·s)
μ_c	Viscosity according to the Casson model (Pa·s)
ν	Cinematic viscosity ($m^2 \cdot s^{-1}$)
ρ	Density ($kg\ m^{-3}$)
σ	Interfacial tension ($N\ m^{-1}$)
τ	Shear stress ($N\ m^{-2}$)
τ_0	Apparent yield stress ($N\ m^{-2}$)
τ_r	Electrode response time (s)

Sub-indexes

ave	Relative to average value
CO_2	Relative to carbon dioxide
Cal	Relative to calculated value
Exp	Relative to experimental value
crit	Relative to critic value
G	Relative to gas phase
L	Relative to liquid phase
m	Relative to cell monolayer
me	Relative to measure by electrode or mean
max	Maximum value
O_2	Relative to oxygen
s	Relative to surfactant

Super-indexes

In	Relative to inlet
Out	Relative to outlet
*	Relative to equilibrium value in each phase
o	Cell free medium

Acknowledgement

This work has been supported by Plan Nacional I+D, Programa de Procesos y Productos Químicos, under contracts no. CTQ2004-06553-C02-01 and CTQ2007-60919/PPQ.

References

Abrardi V, Rover G, Sicardi S, Baldi G, Conti R. Sparged vessels agitated by multiple turbines. Proc Eur Conf Mix 1988;6:329–36.
Akita K, Yoshida F. Gas holdup and volumetric mass transfer coefficient in bubble columns. Ind Eng Chem Process Des Dev 1973;12:76–80.
Albal RS, Shah YT, Shumpe A, Carr NL. Mass transfer in multiphase agitated contactors. Chem Eng J 1983;27:61–80.
Al-Masry WA, Abasaeed AE. On the scale-up of external loop airlift reactors: Newtonians systems. Chem Eng Sci 1998;53:4085–94.
Arjunwadkar SJ, Sarvanan AB, Kulkarni PR, Pandit AB. Gas liquid mass transfer in dual impeller bioreactor. Biochem Eng J 1998;1:99-106.
Arrua LA, McCoy BJ, Smith JM. Gas–liquid mass transfer in stirred tanks. AIChE J 1990;36(11):1768–72.
Badino AC, Facciotti MCR, Schmidell W. Volumetric oxygen transfer coefficients (k_La) in batch cultivations involving non-Newtonian broths. Biochem Eng J 2001;8:111–9.
Bandaiphet C, Prasertsan P. Effect of aeration and agitation rates and scale-up on oxygen transfer coefficient, k_La in exopolysaccharide production from Enterobacter cloacae WD7. Carbohydr Polym 2006;66:216–28.
Baird MHI, Rama NV, Shen ZJ. Oxygen absorption in a baffled tank agitated by delta paddle impeller. Can J Chem Eng 1993;71:195–201.
Barigou M, Greaves M. Gas holdup and interfacial area distributions in a mechanically agitated gas–liquid contactor. Trans IChemE 1996;74:397–405.
Bello RA, Robinson CW, Moo-Young M. Liquid circulation and mixing characteristics of air-lift contactors. Can J Chem Eng 1984;62:573–7.
Benadda B, Ismaili S, Otterbein M. Relation of mechanical power to gas hold-up and mass transfer in an agitated vessel. Chem Eng Technol 1997;20:192–8.
Benbelkacem H, Debellefontaine H. Modeling of a gas–liquid reactor in batch conditions. Study of the intermediate regime when part of the reaction occurs within the film and part within the bulk. Chem Eng Process 2003;42:723–32.
Betts JI, Baganz F. Miniature bioreactors: current practices and future opportunities. Microb Cell Fact 2006;5:1-21.
Bhavaraju SM, Russell TWF, Blanch HW. The design of gas sparged devices for viscous liquid systems. AIChE J 1978;24:454–66.
Blanch HW, Clark DS. Biochemical Engineering. New York: Marcel Dekker; 1996.
Billet R, Schultes M. Predicting mass transfer in packed columns. Chem Eng Technol 1993;16:1–9.
Calderbank PH. The interfacial area in gas–liquid contacting with mechanical agitation. Trans Inst Chem Eng 1958;36:443–63.
Calderbank PH. Physical rate processes in industrial fermentation. Part II — Mass transfer coefficients in gas–liquid contacting with and without mechanical agitation. Trans Inst Chem Eng 1959;37:173–85.
Calderbank PH, Moo-Young MB. The power characteristic of agitators for the mixing of Newtonian and non-Newtonian fluids. Trans Inst Chem Eng 1961;39:337–47.
Calik G, Vural H, Özdamar TH. Bioprocess parameters and oxygen transfer effects in the growth Pseudomonas dacunhae for L-alanine production. Chem Eng J 1997;65:109–16.
Calik P, Yilgör P, Ayhan P, Demir AS. Oxygen transfer effects on recombinant benzaldehyde lyase production. Chem Eng Sci 2004;59:5075–83.
Calik P, Yilgör P, Demir AS. Influence of controlled-pH and uncontrolled-pH operations on recombinant benzaldehyde lyase production by *Escherichia coli*. Enzyme Microb Technol 2006;38:617–27.
Carbajal TI, Tecante A. On the applicability of the dynamic pressure step method for k_La determination in stirred Newtonian and non-Newtonian fluids, culture media and fermentation broths. Biochem Eng J 2004;18:185–92.
Chandrasekharan K, Calderbank PH. Further observations on the scale-up of aerated mixing vessels. Chem Eng Sci 1981;36:819–23.
Chisti Y. Airlif Bioreactors. London: Elsevier Applied Science; 1989.
Chisti Y. Pneumatically agitated bioreactors in industrial and environmental bioprocessing: hydrodynamics, hydraulics, and transport phenomena. Appl Mech Rev 1998;51:33-112.
Chisti Y, Moo-Young M. Communications to the editor: on the calculation of shear rate and apparent viscosity in airlift and bubble column bioreactors. Biotechnol Bioeng 1998;34:1391–2.
Clarke KG, Williams PC, Smit MS, Harrison STL. Enhancement and repression of the volumetric oxygen transfer coefficient through hydrocarbon addition and its influence on oxygen transfer rate in stirred tank bioreactors. Biochem Eng J 2006;28:237–42.
Clarke KG, Correia LDC. Oxygen transfer in hydrocarbon–aqueous dispersions and its applicability to alkane bioprocesses: A review. Biochem Eng J 2008;39:405–29.
Cooper CM, Fernstorm GA, Miller SA. Performance of agitated gas–liquid contactors. Ind Eng Chem 1944;36:504–9.
Costa E, Lucas A, Aguado J, Avila JA. Transferencia de materia en tanques agitados: burbujeo de gases en líquidos newtonianos y no newtonianos. I. Turbinas de 6 paletas y difusor plano. An Quim 1982;78:387–92.
Dai Y, Deng T, Wang J, Xu K. Enhancement of oxygen gas–liquid mass transfer with colloidal gas aphron dispersions. Colloids Surf A 2004;240:165–71.
Danckwerts PV. Significance of liquid-film coefficients in gas absorption. Ind Eng Chem 1951;43:1460–7.
Danckwerts PV. Gas–Liquid Reaction. New York: McGraw-Hill; 1970. p. 239–50.
Danckwerts PV, Gillham AJ. The design of gas absorbers: I. — Methods for predicting rates of absorption with chemical reaction in packed columns, and tests with 11/2in. Raschig rings. Trans Inst Chem Eng 1966;44:T42–54.
Davies SM, Gibilaro LG, Middleton JC, Cooke M, Lynch PM. The application of two novel techniques for mass transfer coefficient determination to the scale up of gas sparged agitated vessels. Proc Eur Conf Mix 1985;5:27–34.
De Jesus MJ, Girard P, Bourgeois M, Baumgartner G, Jacko B, Amstutz H, et al. TubeSpin satellites: a fast track approach for process development with animal cells using shaking technology. Biochem Eng J 2004;17:217–23.
Deckwer WD, Furckhart R, Zoll G. Mixing and mass transfer in tall bubble column. Chem Eng Sci 1974;29:2177–88.
Deckwer WD, Nguyen-Tien K, Kelkar BG, Shah YT. Applicability of axial dispersion model to analyze mass transfer measurement in bubble columns. AIChE J 1983;29:915–22.
Dhanasekharan KM, Sanyal J, Jain A, Haidari A. A generalized approach to model oxygen transfer in bioreactors using population balances and computational fluid dynamics. Chem Eng Sci 2005;60:213–8.
Djelal H, Larher F, Martin G, Amrane A. Effect of the dissolved oxygen on the bioproduction of glycerol and ethanol by Hansenula anomala growing under salt stress conditions. J Biotechnol 2006;125:95-103.
Doig SD, Diep A, Baganz F. Characterisation of a novel miniaturised bubble column bioreactor for high throughput cell cultivation. Biochem Eng J 2005;23:97-105.
Duetz WA, Ruedi L, Hermann R, O'Connor K, Buchs J, Witholt B. Methods for intense aeration, growth, storage and replication of bacterial strains in microtiter plates. Appl Environ Microbiol 2000;66:2641–6.
Duetz WA, Witholt B. Oxygen transfer by orbital shaking of square vessels and deepwell microtiter plates of various dimensions. Biochem Eng J 2004;17:181–5.
Dumon E, Delmas H. Mass transfer enhancement of gas absorption in oil-in-water systems: a review. Chem Eng Process 2003;42:419–38.
Dussap CG, Decorps J, Gros JB. Transfert d'oxygene en presence de polysaccharides exocellulaires dans un fermenteur agite aeré et dans un fermenteur de type gazosiphon. Entropie 1985;123:11–20.
Eickenbusch H, Brunn PO, Schumpe A. Mass transfer into viscous pseudo-plastic liquid in large-diameter bubble columns. Chem Eng Process 1995;34:479–85.
Figueiredo LM, Calderbank PH. The scale-up of aerated mixing vessels for specified oxygen dissolution rates. Chem Eng Sci 1979;34:1333–8.
Flickinger MC, Greenstein M, Bremmon C, Colin J. Strain selection, medium development and scale-up to toyocamycin production by *Streptomyces chrestomyceticus*. Bioprocess Eng 1990;5:143–53.
Fukuma M, Muroyama K, Yasunishi A. Specific gas–liquid interfacial area and liquid-phase mass transfer coefficient is a slurry bubble column. J Chem Eng Jpn 1987;20:321–4.

Gagnon H, Lounes M, Thibault J. Power consumption and mass transfer in agitated gas–liquid columns: A comparative study. Can J Chem Eng 1998;76:379–89.
Galaction AI, Cascaval D, Onisco C, Turnea M. Prediction of oxygen mass transfer coefficients in stirred bioreactors for bacteria, yeast and fungus broths. Biochem Eng J 2004;20:85–94.
Galindo E, Flores C, Larralde-Corona P, Corkidi-Blanco G, Rocha-Valadez JA, Serrano-Carreón L. Production of 6-pentyl-α-pyrone by Trichoderma harzianum cultured in unbaffled and baffled shake flasks. Biochem Eng J 2004;18:1–8.
Garcia Camacho F, Gallardo Rodriguez JJ, Sanchez Miron A, Ceron Garcia MC, Belarbi EH, Molina Grima E. Determination of shear stress thresholds in toxic dinoflagellates cultured in shaken flasks Implications in bioprocess engineering. Process Biochem 2007;42:1506–15.
Garcia-Calvo E. A fluid dynamic model for airlift reactors. Chem Eng Sci 1989;44:321–3.
Garcia-Calvo E. Fluid dynamic of airlift reactors: two-phase friction factors. AIChE J 1992;38:1662–6.
Garcia-Calvo E, Leton P. A fluid dynamic model for bubble column and airlift reactors. Chem Eng Sci 1991;46:2947–51.
Garcia-Calvo E, Rodriguez A, Prados A, Klein J. Fluid dynamic model for three-phase airlift reactors. Chem Eng Sci 1999;54:2359–70.
Garcia-Ochoa F, Gomez E. Mass transfer coefficient in stirrer tank reactors for xanthan solutions. Biochem Eng J 1998;1:1-10.
Garcia-Ochoa F, Gomez E. Estimation of oxygen mass transfer coefficient in stirrer tank reactors using artificial neuronal networks. Enzyme Microb Technol 2001;28:560–9.
Garcia-Ochoa F, Gomez E. Theoretical prediction of gas–liquid mass transfer coefficient, specific area and hold-up in sparged stirred tanks. Chem Eng Sci 2004;59:2489–501.
Garcia-Ochoa F, Gomez E. Prediction of gas–liquid mass transfer in sparged stirred tank bioreactors. Biotechnol Bioeng 2005;92:761–72.
Garcia-Ochoa F, Gomez E, Santos VE. Oxygen transfer and uptake rates during xanthan gum production. Enzyme Microb Technol 2000a;27:680–90.
Garcia-Ochoa F, Santos VE, Casas JA, Gomez E. Xanthan gum: production, recovery, and properties. Biotechnol Adv 2000b;18:549–79.
Gauthier L, Thibault J, LeDuy A. Measuring k_La with randomly pulsed dynamic method. Biotechnol Bioeng 1991;37:889–93.
Gill NK, Appleton M, Baganz F, Lye GJ. Design and characterisation of a miniature stirred bioreactor system for parallel microbial fermentations. Biochem Eng J 2008;39: 164–76.
Godbole SP, Shumpe A, Shah YT, Carr NL. Hydrodynamics and mass transfer in non-Newtonian solutions in a bubble column. AIChE J 1984;30:213–20.
Gogate PR, Beenackers AACM, Pandit AB. Multiple-impeller systems with a special emphasis on bioreactors: a critical review. Biochem Eng J 2000;6:109–44.
Gomez, E. Transferencia de oxígeno en biorreactores tipo tanque agitado: Aplicación a la producción de xantano. PhD Thesis. Madrid, Spain: Universidad Complutense Madrid, 1995.
Gomez E, Santos VE, Alcon A, Garcia-Ochoa F. Oxygen transport rate on *Rhodococcus erythropolis* cultures: Effect on growth and BDS capability. Chem Eng Sci 2006;61: 4595–604.
Gourich B, Vial CH, El Azher N, Belhaj Soulami M, Ziyad M. Influence of hydrodynamics and probe response on oxygen mass transfer measurements in a high aspect ratio bubble column reactor: Effect of the coalescence behaviour of the liquid phase. Biochem Eng J 2008;39:1-14.
Hermann C, Dewes I, Shumpe A. The estimation of gas solubilities in salt solutions. Chem Eng Sci 1995;50:1673–5.
Johnson J, Andre G, Chavarie C, Archambault J. Oxygen transfer rate in a mammalian cell culture bioreactor equipped with a cell-lift impeller. Biotechnol Bioeng 1990;35:43–9.
Ju LK, Sundararajan A. Model analysis of biological oxygen transfer enhancement in surface-aerated bioreactors. Biotechnol Bioeng 1992;40:1343–52.
Halard B, Kawase Y, Moo-Young M. Mass transfer in a pilot plant scale airlift column with non-Newtonian fluids. Ind Eng Chem Res 1989;28:243–5.
Herbst H, Shumpe A, Deckwer WD. Xanthan production in stirred tank fermenters: oxygen transfer and scale-up. Chem Eng Technol 1992;15:425–34.
Higbie R. The rate of absorption of a pure gas into a still liquid during short periods of exposure. Inst Chem Eng 1935;35:36–60.
Hill GA. Measurement of overall volumetric mass transfer coefficients for carbon dioxide in well-mixed reactor using a pH probe. Ind Eng Chem Res 2006;45:5796–800.
Hiraoka S, Kato Y, Tada Y, Kai S, Inoue N, Ukai Y. Power consumption and gas–liquid mass transfer volumetric coefficient in a mechanically agitated vessel with wire-gauze impeller. J Chem Eng Jpn 2001;34:600–5.
Höcker H, Langer G, Werner U. Mass transfer in aerated Newtonian and non-Newtonian liquids in stirred reactors. Ger Chem Eng 1981;4:51–62.
Hughmark GA. Holdup and mass transfer in bubble columns. Ind Eng Chem Process Des Dev 1967;6:218–20.
Jackson ML, Shen CC. Aeration and mixing in deep tank fermentation systems. AIChE J 1978;24:63–71.
Johnson AI, Huang C. Mass transfer studies in an agitated vessel. AIChE J 1956;2:412–9.
Joshi JB, Pandit AB, Sharma MM. Mechanically agitated gas–liquid reactors. Chem Eng Sci 1982;37:813–44.
Ju LK, Chase GG. Improved scale-up strategies of bioreactors. Bioprocess Eng 1992;8: 49–53.
Junker BH. Scale-up methodologies for *Escherichia coli* and yeast fermentation processes. J Biosci Bioeng 2004;97:347–64.
Kantarci N, Borak F, Ulgen KO. Bubble column reactors. Process Biochem 2005;40: 2263–83.
Kato I, Tanaka H. Development of a novel Box-Shaped shake flask with efficient gas exchange capacity. J Ferment Bioeng 1998;85:404–9.
Kawase Y, Hashiguchi N. Gas–liquid mass transfer in external-loop airlift columns with Newtonian and non-Newtonian fluids. Chem Eng J 1996;62:35–42.
Kawase Y, Moo-Young M. Volumetric mass transfer coefficients in aerated stirred tank reactors with Newtonian and non-Newtonian media. Chem Eng Res Dev 1988;66: 284–8.
Kawase Y, Moo-Young M. Mathematical models for design of bioreactors: applications of Kolmogoroff's theory of Isotropic Turbulence. Chem Eng J 1990;43:B19-41.
Kawase Y, Halard B, Moo-Young M. Theoretical prediction of volumetric mass transfer coefficients in bubble columns for Newtonian and non-Newtonian fluids. Chem Eng Sci 1987;42:1609–17.
Kawase Y, Halard B, Moo-Young M. Liquid-phase mass transfer coefficients in bio-reactors. Biotechnol Bioeng 1992a;39:1133–40.
Kawase Y, Umeno S, Kumagai T. The prediction of gas hold-up in bubbles column reactors: Newtonian and non-Newtonian fluids. Chem Eng J 1992b;50:1–7.
Kieran PM, Malone DM, MacLoughlin PM. Effects of hydrodynamic and interfacial forces on plant cell suspension systems. On: influence of stress on cell growth and product formation. Adv Biochem Eng Biotechnol 2000;67:139–77.
Kilonzo PM, Margaritis A. The effects of non-Newtonian fermentation broth viscosity and small bubble segregation on oxygen mass transfer in gas-lift bioreactors: a critical review. Biochem Eng J 2004;17:27–40.
Kudrewizki F. Zur Berechung des gasgehaltes in begasten Rührkesseln. Chem Technol 1982;34:247–9.
Kudrewizki F, Rabe P. Model of the dissipation of mechanical energy in gassed stirred tanks. Chem Eng Sci 1986;41:2247–52.
Lamont JC, Scott DS. An eddy cell model of mass transfer into the surface of a turbulent liquid. AIChE J 1970;16:513–9.
Lamping SR, Zhang H, Allen B, Shamlou PA. Design of a prototype miniature bioreactor for high throughput automated bioprocessing. Chem Eng Sci 2003;58: 747–58.
Letzel HM, Schouten JC, Krishna R, Van Den Bleek CM. Gas hold-up and mass transfer in bubble column reactors operated at elevated pressure. Chem Eng Sci 1999;54: 2237–46.
Li GG, Yan SZ, Cai ZL, Chen JY. Mass transfer and gas–liquid circulation in an airlift bioreactor with viscous non-Newtonian fluids. Chem Eng J 1995;56:B101-107.
Li X, van der Steen G, van Dedem GWK, van der Wielen LAM, van Leeuwen M, van Gulik WM, et al. Improving mixing in microbioreactors. Chem Eng Sci 2008;63: 3036–46.
Linek V, Vacek V. Volumetric mass transfer coefficient in stirred reactors. Chem Eng Technol 1981a;11:249–51.
Linek V, Vacek V. Chemical engineering use of catalyzed sulfite oxidation kinetics for the determination of mass transfer characteristics of gas–liquid contactors. Chem Eng Sci 1981b;36:1747–68.
Linek V, Sinkule J, Benes P. Critical assessment of gassing-in method measuring k_La in fermentors. Biotechnol Bioeng 1991;38:323–30.
Linek V, Moucha T, Dousova M, Sinkule J. Measurent of k_La by dynamic pressure method in pilot-plant fermentor. Biotechnol Bioeng 1994;43:477–82.
Linek V, Kordac M, Moucha T. Mechanism of mass transfer from bubbles in dispersions. Part II: Mass transfer coefficients in stirred gas–liquid reactor and bubble column. Chem Eng Process 2005;44:121–30.
Liu YS, Wu JY, Ho K-p. Characterization of oxygen transfer conditions and their effects on Phaffia rhodozyma growth and carotenoid production in shake-flask cultures. Biochem Eng J 2006a;27:331–5.
Liu T, Miura S, Yaguchi M, Arimura T, Park EY, Okabe M. Scale-up of L-Lactic acid production by mutant strain *Rhizopus* sp. MK-96-1196 from 0.003 m^3 to 5 m^3 in airlift bioreactors. J Biosci Bioeng 2006b;101:9-12.
Margaritis A, Zajic JE. Biotechnology review: mixing, mass transfer and scale-up of polysaccharide fermentations. Biotechnol Bioeng 1978;20:939-1001.
Martin AB, Alcon A, Santos VE, Garcia-Ochoa F. Production of a biocatalyst of Pseudomonas putida CECT5279 for DBT biodesulphurization: influence of the operational conditions. Biochem Eng J 2005;22:229–37.
Masiuk S, Lacki H, Strek F. Power consumption and mixing times for liquid mixing in a ribbon mixer. Chem Eng J 1992;48:135–40.
Merchuk JC. Further considerations on the enhancement of oxygen transfer in fermentation broths. Biotechnol Bioeng 1977;19:1885–9.
Merchuk JC. Hydrodynamics and holdup in air-lift reactors. In: Cheremisinoff NP, editor. Encyclopedia of Fluid Mechanics.Vol.3, Chap.41. Gulf. Publ. Co.; 1986
Merchuk JC, Gluz M. Airlift reactors. In: Flickinger MC, Drew SW, editors. Encyclopedia of Bioprocess Technology. New York: John Wiley & Sons; 1999. p. 320–53.
Merchuk JC, Yona S, Siegel MH, Ben Zvi A. On the first-order approximation to the response of dissolved oxygen electrodes for dynamic KLa estimation. Biotechnol Bioeng 1990;35:1161–3.
Merchuk JC, Ladwa N, Cameron A, Bulmer M, Pickett A. Concentric-tube airlift reactors: Effects of geometrical design on performance. AIChE J 1994;40:1105–17.
Michel BJ, Miller SA. Power requirements of gas–liquid agitated systems. AIChE J 1962;8:262–7.
Micheletti M, Barret T, Doig SD, Baganz F, Levy MS, Woodley JM, et al. Fluid mixing in shaken bioreactors: Implications for scale-up predictions from microliter-scale microbial and mammalian cell cultures. Chem Eng Sci 2006;61:2939–49.
Mignone CF. The agitation-step method for k_La measurement. Chem Eng Sci 1990;45: 1583–7.
Nakanoh M, Yoshida F. Gas absorption by Newtonian and non-Newtonian liquids in a bubble column. Ind Eng Chem Process Des Dev 1980;19:190–5.
Nedeltchev S, Ookawara S, Ogawa K. A fundamental approach to bubble column scale-up based on quality of mixedness. J Chem Eng Jpn 1999;32:431–9.
Nedeltchev S, Jordan U, Schumpe A. Correction of the penetration theory based on mass transfer data from bubble columns operated in the homogeneous regime under high pressure. Chem Eng Sci 2007;62:6263–73.
Netusil J, Rieger F. Power consumption of screw and helical ribbon agitators in highly viscous pseudo-plastic fluids. Chem Eng J 1993;52:9-12.

Nishikawa M, Nakamura M, Yagi H, Hashimoto K. Gas absorption in aerated mixing vessels. J Chem Eng Jpn 1981;14:219–26.
Nocentini M, Fajner D, Pasquali G, Magelli F. Gas–liquid mass transfer and holdup in vessels stirred with multiple rushton turbines: water and water-glycerol solutions. Ind Eng Chem Res 1993;32:19–26.
Novak M, Klekner V. Comparison of various methods of K_La estimation in cultures of filamentous microorganisms. Biotechnol Techn 1988;2:243–8.
Oldshue JY. Fermentation mixing scale-up techniques. Biotechnol Bioeng 1966; VIII:3-24.
Olmo CH, Santos VE, Alcon A, Garcia-Ochoa F. Production of a *Rhodococcus erythropolis* IGTS8 biocatalyst for DBT biodesulphurization: influence of operational conditions. Biochem Eng J 2005;22:229–37.
Ogut A, Hatch RT. Oxygen transfer Newtonian and non-Newtonian fluids in mechanically agitated vessels. Can J Chem Eng 1988;66:79–85.
Onken U, Sick R, Weiland P. Determination of gas–liquid mass transfer by oxidation of hydrazine. Chem Eng Sci 1985;40:1990–3.
Ortiz-Ochoa K, Doig SD, Ward JM, Baganz F. A novel method for the measurement of oxygen mass transfer rates in small-scale vessels. Biochem Eng J 2005;25:63–8.
Parthasarathy R, Jameson GJ, Ahmed N. Bubble breakup in stirred vessels-predicting the Sauter mean diameter. Trans Inst Chem Eng 1991;69:295–301 Part A.
Pedersen AG, Andersen H, Nielsen J, Villadsen J. A novel technique based on Kr-85 for quantification of gas–liquid mass transfer in bioreactors. Chem Eng Sci 1994;6: 803–10.
Perez JF, Sandall OC. Gas absorption by non-Newtonian fluids in agitated vessels. AIChE J 1974;20:770–5.
Peter CP, Suzuki Y, Rachinskiy K, Lotter S, Büchs J. Volumetric power consumption in baffled shake flasks. Chem Eng Sci 2006;61:3771–9.
Popovic MK, Robinson CW. Mass transfer studies of external-loop airlifts and a bubble column. AIChE J 1989;35:393–405.
Prasher BD, Wills GB. Mass transfer in agitated vessel. Ind Eng Chem Process Des Dev 1973;12:351–4.
Puthli MS, Rathod VK, Pandit AB. Gas–liquid mass transfer studies with triple impeller system on a laboratory scale bioreactor. Biochem Eng J 2005;23:25–30.
Rushton JH, Costich EW, Everett HJ. Power characteristics of mixing impeller. Chem Eng Prog 1950;46:395–404.
Sanchez A, Garcia F, Contreras A, Molina E, Chisti Y. Bubble-column and airlift photobioreactors for algal culture. AIChE J 2000;46:1872–87.
Schlüter V, Deckwer WD. Gas/liquid mass transfer in stirred vessels. Chem Eng Sci 1992;47:2357–62.
Schügerl K, Lübbert A. Pneumatically Agitated Bioreactors. In: Asenjo JA, Merchuk JC, editors. Bioreactors System Design. New York; 1995. p. 257–303.
Sharma MM, Danckwerts PV. Chemical methods of measuring interfacial area and mass transfer coefficients in two-fluid systems. Br Chem Eng 1970;15:522–7.
Shimizu K, Takada S, Minekawa K, Kawase Y. Phenomenological model for bubble column reactors: prediction of gas hold-ups and volumetric mass transfer coefficients. Chem Eng J 2000;78:21–8.
Shimizu K, Takada S, Takahashi T, Kawase Y. Phenomenological simulation model for gas hold-ups and volumetric mass transfer coefficients in external-loop airlift reactors. Chem Eng J 2001;84:599–603.
Shukla VB, Veera UP, Kulkarni PR, Pandit AB. Scale up of biotransformation process in stirred tank reactor using dual impeller bioreactor. Biochem Eng J 2001;8:19–29.
Suh IS, Schumpe A, Deckwer WD, Kulicke WM. Gas–liquid mass transfer in the bubble column with viscoelastic liquid. Can J Chem Eng 1991;69:506–12.
Suh IS, Schumpe A, Deckwer WD. Xanthan production in bubble column and air-lift reactors. Biotechnol Bioeng 1992;39:85–94.
Taguchi H, Humphrey AE. Dynamic Measurement of the volumetric oxygen transfer coefficient in fermentation systems. J Ferment Technol 1966;44:881–9.
Thibault J, Leduy A, Denis A. Chemical enhancement in the determination of k_La by the sulfite oxidation method. Can J Chem Eng 1990;68:324–6.
Tobajas M, Garcia-Calvo E, Siegel MH, Apitz SE. Hydrodynamics and mass transfer prediction in a three-phase airlift reactor for marine sediment biotreatment. Chem Eng Sci 1999;54:5347–54.
Toor HL, Marchelo JM. Film-penetration model for mass transfer and heat transfer. AIChE J 1958;4:97-101.
Tsao GT. Simultaneous gas–liquid interfacial mass transfer and uptake by small particles. Biotechnol Bioeng 1969;11:1071–87.
Van der Meer AB, Beenackers AACM, Burghard R, Mulder NH, Fok JJ. Gas/liquid mass transfer in a four-phase stirred fermentor: effects of organic phase hold-up and surfactant concentration. Chem Eng Sci 1992;47:2369–74.
Uchida S, Tsuyutani S, Seno T. Flow regimes and mass transfer in counter-current bubble columns. Can J Chem Eng 1989;67:866–9.
Van Swaaij WPM, Versteeg GF. Mass transfer accompanied with complex reversible chemical reactions in gas–liquid systems. An overview. Chem Eng Sci 1992;47: 3181–95.
Van't Riet K. Review of measuring methods and nonviscous gas–liquid mass transfer in stirred vessels. Ind Eng Chem Process Des Dev 1979;18:357–64.
Vasconcelos JMT, Orvalho SCP, Rodríguez AM, Alves SS. Effect of blade shape on the performance of six blade disk turbine impellers. Ind Eng Chem Res 2000;39:203–8.
Vasconcelos JMT, Alves SS, Nienow AW, Bujalski W. Scale-up of mixing in gassed multi-turbine agitate vessels. Can J Chem Eng 1998;76:398–403.
Vasconcelos JMT, Rodrigues JMI, Orvalho SCP, Alves SS, Mendes RL, Reis A. Effect of contaminants on mass transfer coefficients in column and airlift contactors. Chem Eng Sci 2003;58:1431–40.
Vashitz O, Sheintuch M, Ulitzur S. Mass studies using cloned-luminous strain of *Xanthomonas campestris*. Biotechnol Bioeng 1989;34:671–80.
Vatai GY, Tekic MN. Gas hold-up and mass transfer in bubble columns with pseudo-plastic liquids. Chem Eng Sci 1989;44:2402–7.
Wang DIC, Cooney CL, Demain AL, Dunnill P, Humphrey AE, Lilly MD. Aeration and Agitation. Fermentation and enzyme technology. New York: John Wiley & sons; 1979. Chapter 9, 157–193.
Weiland P, Onken U. Fluid dynamics and mass transfer in an airlift fermenter with external loop. Ger Chem Eng 1981;4:42–50.
Weissenborn PK, Pugh RJ. Surface tension of aqueous solutions of electrolytes: relationship with ion hydration, oxygen solubility, and bubble coalescence. J Colloid Interface Sci 1996;184:550–63.
Whitman WG. Preliminary experimental confirmation of the two-film theory of gas absorption. Chem Metall Eng 1923;29:146–9.
Wilkinson PM, Haringa H, Van Dierendonck LL. Mass transfer and bubble size in bubble column under pressure. Chem Eng Sci 1994;49:1417–27.
Yagi H, Yoshida F. Oxygen absorption in fermenters — effects of surfactants, antifoaming agents, and sterilized cells. J Ferment Technol 1974;52:905–16.
Yagi H, Yoshida F. Gas absorption by Newtonian and non-Newtonian fluids in sparged agitated vessels. Ind Eng Chem Process Des Dev 1975;14:488–93.
Yang JD, Wang NS. Oxygen mass transfer enhancement via fermentor headspace pressurization. Biotechnol Prog 1992;8:244–51.
Yasukawa M, Onodera M, Yamagiwa K, Ohkawa A. Gas holdup, power consumption, and oxygen absorption coefficient in a stirred-tank fermentor under foam control. Biotechnol Bioeng 1991;38:629–36.
Zhan T, Wang T, Wang J. Analysis and measurement of mass transfer in airlift loop reactors. Chin J Chem Eng 2006;14:604–10.
Zhang Z, Thomas CR. Eddy number distribution in isotropic turbulence and its application for estimating mass transfer coefficients. Chem Eng Commun 1996;140:207–17.
Zhang Z, Perozziello G, Boccazzi P, Sinskey AJ, Geschke O, Jensen KF. Microbioreactors for Bioprocess Development. J Assoc Lab Autom 2007;12:143–51.
Zhu Y, Bandopadhayay PC, Wu J. Measurement of gas–liquid mass transfer in an agitated vessel — a comparison between different impellers. J Chem Eng Jpn 2001;34:579–84.
Znad H, Báles V, Markos J, Kawase Y. Modelling and simulation of airlift bioreactors. Biochem Eng J 2004;21:73–81.